Technical Report Documentation Page

1. Report No. Research Report RC-1466	2. Government Accession No.	3. MDOT Project Manager Roger Till
4. Title and Subtitle LRFD Load Calibration for State of Michigan Trunkline Bridges		5. Report Date August 1, 2006
7. Author(s) Gongkang Fu (WSU), John W. van de Lindt (CSU), Shiling Pei (CSU),Reynaldo M. Pablo Jr (WSU), and Saharat Buddhawanna (CSU)		6. Performing Organization Code MTU/WSU
9. Performing Organization Name and Address Wayne State University Detroit, MI 48202 Colorado State University Fort Collins, CO 80523-1372		8. Performing Org Report No.
12. Sponsoring Agency Name and Address Michigan Department of Transportation Construction and Technology Division P.O. Box 30049 Lansing, MI 48909		10. Work Unit No. (TRAIS) 11. Contract Number: 2002-0546-WSU; 2003-0063-MTU 11(a). Authorization Number: WSU-1, MTU-1
15. Supplementary Notes		13. Type of Report & Period Covered Final Report, 2003-2006 14. Sponsoring Agency Code

16. Abstract

This report presents the process and results of a research effort to calibrate the live load factor for the load and resistance factor (LRFD) design of bridges on Michigan's trunkline roadways. Initially, the AASHTO LRFD Bridge Code was reviewed which included investigation into the design code's background documentation (NCHRP Report 368). Weigh-in-motion (WIM) data were procured for more than 100 million trucks at sensor locations throughout the state of Michigan, including those gathered by other researchers earlier. The WIM data were divided by functional classification and numerically run over influence lines for 72 different critical load effects present on 20 randomly selected bridges, and then projected to create the statistical distribution of the 75-year maximum . Several projection techniques were investigated for comparison. Projection using the Gumbel approach presented herein was found to be the most theoretically accurate for the data set. However, taking into account the practical approach used in the calibration of the AASHTO LRFD Bridge Code, a more empirical and consistent approach was selected for application. Based on the findings presented herein and those of the Phase I portion of this study, the live load factor was calibrated using an approach that was as consistent as possible with that used for the AASHTO LRFD Bridge Code calibration. A reliability index β of 3.5 was used as the structural safety target in both calibrations. Based on the calibration results herein, it is recommended that the live load factor should be increased by a factor of 1.2 for the Metro Region in Michigan to cover observed heavy truck loads. For other regions in the state, this additional factor is not needed. The cost impact of this recommended change was also studied and documented in this report, and was estimated at a 4.5% cost increase for the Metro Region only.

17. Key Words: Structural reliability, design load, bridge design, capacity, resistance, reliability index, LRFD	18. Distribution Statement No restrictions. This document is available to the public through the Michigan Department of Transportation.

19. Security Classification (report) Unclassified	20. Security Classification (Page) Unclassified	21. No of Pages 63	22. Price

Report RC-1466

LRFD Load Calibration for State of Michigan Trunkline Bridges

Submitted jointly by:

Gongkang Fu (WSU) and John W. van de Lindt (CSU)

Final Report – August 2006

Acknowledgements

This research project was funded by the Michigan Department of Transportation (MDOT) with the cooperation of the Federal Highway Administration. Their support is gratefully acknowledged.

During the course of this study, many MDOT personnel provided direction and assistance. Specifically, the Project Manager Roger Till and the members of the Technical Advisory Group (TAG). Jon Nekritz from FHWA also provided valuable assistance and guidance during the course of the project. Without their efforts, this project would not have been successfully completed.

Shiling Pei and Saharat Buddhawanna, Ph.D. candidates at Colorado State University, organized and processed all of the live load data and also performed calculation of the bridge reliability indices. Reynaldo Pablo and several other graduate research assistants with Wayne State University ably assisted in analysis and data acquisition reported herein. Their assistance is gratefully acknowledged.

Disclaimer

Table of Contents

Chapter 1: Introduction

1.1 Background

The load carrying capacity of bridges is strongly influenced by the design load used in their design. The design load also has a significant effect on the durability of these bridges. Traditionally, the design load adopted in the design specifications is applied uniformly within the jurisdiction of a transportation agency, with some exception. For example, a state typically uses one design load level for most bridge designs in the state, with a possible exception for bridges that have a particular function or characteristic that may warrant a different design load, such as those on certain local roads. This practice has been justifiable in that it reduces required engineering design work and avoids bridge-specific design-load. On the other hand, this approach also neglects location-specific truck loads that may be substantially different from bridge to bridge.

This issue may become critical when the actual truck loads are noticeably higher than the design load. The motivation for this project was that bridges experiencing these higher loads are subjected to a higher risk of distress, damage, and even failure.

In 1972 the Michigan Department of Transportation (MDOT) changed the design load level for all bridges located on Interstate and Arterial highways from HS20 to HS25. Currently MDOT still uses the HS25 load for beam design and the HS20 axle load for deck design. Note that the HS25 load is used in many other states. However, MDOT will be moving to the HL93 load configuration, which is part of the AASHTO LRFD Bridge Code (AASHTO 1998), as mandated by the Federal Highway Administration. Several other changes to the design loading and calculated resistances are present in the AASHTO LRFD Bridge Code and are also addressed in this report.

An MDOT research report, Report RC-1413 (van de Lindt et al., 2002) systematically demonstrated that the HS25 design load used in the state of Michigan did not consistently provide a reliability index compatible[Seems redundant as written.] with that used as the target for the AASHTO LRFD bridge code. The reader is referred to MDOT Research Report RC-1413 for more background information.

1.2 Objective, Approach, and Scope of Research

The objective of this research project is to determine what scaling of the HL93 bridge design load configuration will provide Michigan's truckline bridges designed using the LRFD bridge design code a consistent reliability index of 3.5. The need for this is based on (1) the state's heavy truck loads, and (2) the results of Phase 1 outlined previously in section 1.1 of this report.

Structural safety is measured in this study using the structural reliability index β. This approach has been used in several recent research projects related to bridge safety. The previous research most relevant to the present project is NCHRP Project 12-33: Development of LRFD Bridge Design Specifications (Nowak 1999) and MDOT Research Report RC-1413: Investigation of the Adequacy of Current Bridge Design Loads in the State of Michigan (van de Lindt et al., 2002). In NCHRP Project 12-33, the LRFD bridge design code was calibrated with respect to structural safety, which was also measured using the reliability index β. This was the first time the concept of structural safety was used in the AASHTO specifications. While more details about the definition and calculation of β are given in Section 1.3, it is noted here that a large β indicates a higher safety level and a lower β a lower safety level.

For evaluation of the design load, this research effort covers only the bridge superstructure. The design load is examined in the context of the load and resistance factor design (LRFD) method contained in the AASHTO LRFD Bridge Design specifications (1998).

A survey of the state bridge inventory conducted by the authors found that the following four superstructure types represent 91% of the new bridges built between 1991 and 2001 in Michigan. 1.) Steel beam bridges (40.0%). 2.) Prestessed concrete I beam bridges (30.6%). 3.) Adjacent prestressed concrete box beam bridges (14.6%). 4.) Spread prestressed box beam bridges (5.6%). Accordingly, these four bridge superstructure types are covered in the present study, because they represent the population of new bridges in the state for foreseeable future. Each of these bridge types has a configuration of concrete-deck–supported-by-beams. For each of these four types, 5 bridges were randomly selected from those built in the past 10 years. This sample of 20 bridges was used in this study to represent the new bridge population in Michigan, particularly to provide information on dead loads, span lengths, etc., for the reliability analyses. No bridges designed using the AASHTO LRFD (1998) and located in Michigan were available for use in this study.

Structural reliability analysis was performed for the interior beams for each of these randomly selected bridges, as well as for the reinforced concrete decks. For the beams, both moment and shear effects are covered.

1.3 Structural Reliability Index β as A Measurement of Bridge Safety

In this research project, the structural safety of a structural component is evaluated using its failure probability defined as follows.

$$\text{Failure Probability} = P_f = \text{Probability}\,[\,\text{Resistance} - \text{Load Effect} < 0\,]$$

$$= \text{Probability}\,[\,R - Q < 0\,] \qquad (1\text{-}1)$$

where resistance R is the load carrying capacity of the structural component, and load effect, Q, is the load demand on the component. For example, the load effect can be bending moment for a beam section and the resistance is the beam section's moment capacity. The resistance and load effect in Equation 1-1 are modeled as random variables because they both possess an amount of uncertainty. In general, the uncertainties associated with the resistance are due to material properties and the production and preparation process, construction quality, etc. The uncertainty associated with load effect is related to truck weight, truck type, traffic volume, etc. Note that the failure probability in Equation 1-1 refers to a load effect in a structural component. Namely, this definition can be applied to a variety of load effects, such as moment, shear, or even possibly displacement if this serviceability is an issue. It also can be applied to a variety of bridge structural components, such as beams, slabs, piers, etc.

The reliability index β can be expressed in terms of the failure probability given in equation 1-1 as

$$\beta = \Phi^{-1}\left(1 - P_f\right) \qquad (1\text{-}2)$$

where function Φ^{-1} is the inverse function of the standard normal random variable's cumulative distribution function. Calculation of this function has become a routine in a number of commercially available computer programs. For example in Microsoft Excel, this function is symbolized as NORMSINV. Equation 1-2 indicates that β is inversely monotonic (i.e. β increases with decreasing P_f) with P_f. Namely, a small P_f leads to a large β, or a large P_f to a small β. Thus a large β indicates a safer

structural component and a small β a less safe one. Table 1-1 shows this relationship between β and P_f for a range of different levels.

Table 1-1: Probability of failure levels corresponding to various reliability indices

β	P_f
1.0	0.159
1.5	0.067
2.0	0.023
2.5	0.0062
3.0	0.0013
3.5	0.000233
4.0	0.0000317
4.5	0.0000034
5.0	0.00000029
7.0	0.00000000000128
8.0	0.000000000000000666

When the resistance and load effect can be modeled as normal random variables independent of each other, the safety margin

$$Z = R - Q \tag{1-3}$$

is then also a normal random variable. In this case the reliability index β can be more easily expressed as

$$\beta = \frac{\mu_Z}{\sigma_Z} \tag{1-4}$$

where μ_Z and σ_Z are the mean and the standard deviation of random variable Z. They can be computed as

$$\mu_Z = \mu_R - \mu_Q \tag{1-5a}$$

$$\sigma_Z = \left(\sigma_R^2 + \sigma_Q^2\right)^{1/2} \tag{1-5b}$$

where μ and σ are symbols for the mean and standard deviation, and subscripts R and Q indicate the random variables referenced. Thus, substituting equation 1-5 into equation 1-4 leads to

$$\beta = \frac{\left(\mu_R - \mu_Q\right)}{\sqrt{\sigma_R^2 + \sigma_Q^2}} \tag{1-6}$$

Note that a more general definition of the reliability index β in the literature is given in a U-space of standardized normal variables (instead of the basic random variables as R and Q in this problem) (Madsen et al 1986) and is explained below. The standardized normal random variables have a mean of 0 and standard deviation of 1. In this more general definition, β is defined as the shortest distance from the

origin (0,0) to the failure surface Z=0, in the U-space. The following explains this general definition using the example defined in equation 1-3.

In this example, the basic random variables are R and Q. The U-space of standardized normal variables can then be constructed as follows. The normal random variable X_R standardized from R is defined as

$$X_R = \frac{(R - \mu_R)}{\sigma_R} \tag{1-7a}$$

and the normal variable X_Q standardized from Q is defined similarly as

$$X_Q = \frac{(Q - \mu_Q)}{\sigma_Q} \tag{1-7b}$$

where μ and σ are symbols for the mean and standard deviation as defined earlier. The definition of X_R and X_Q in equation 1-7 is such that they have mean value 0 and standard deviation of 1. In the U-space spanned by the standardized normal variables (X_R and X_Q in this example), the origin is located at the mean values of the random variables, namely (0,0) in this example.

In the U-space, the failure surface $Z = 0$ must also be transformed from its original space (Equation 1-3 in this example). Through substitution of equations 1-7a and 1-7b into equation 1-3, Z can be expressed as

$$Z = \sigma_R X_R + \mu_R - \sigma_Q X_Q - \mu_Q \quad = 0 \tag{1-8}$$

The reliability index β is then defined in this standardized U space as the shortest distance from the origin to the failure surface $Z = 0$. Figure1-1 presents the U space for this example defined using the two standardized random variables X_R and X_Q. The entire space is divided into two halves by the failure surface Z=0. The top right half space above the failure surface (Z=0) is defined by Z<0. This represents a region where the structural component fails. This region is marked as “failure region” as shown. In contrast, the bottom left half space below Z = 0, marked “safe region”, represents a region where the structural component is safe. In this region, Z >0. For this simple example of a linear failure surface as defined in equation 1-8, it can be shown by derivation that in the U-space the reliability index β is given by equation 1-6, where β is the shortest distance from the origin (0,0) to the failure surface (Z=0). Thus, Equation 1-6 can be viewed as a special case for this more general definition of β in the U-space. This β value is also indicated in Figure 1-1. Note also that the point where β is measured from the origin is referred to as the design point, as shown in Figure 1-1.

In general, the failure surface Z = 0 can be nonlinear, i.e., not linear as in this example. When this is the case, the failure surface may be linearized to provide an approximation for simplicity of computation. This simplification does not significantly sacrifice accuracy if the failure surface Z=0 is not highly nonlinear at the design point. When this linearization is performed using numerical methods, the resulting linearized failure surface is then used as the failure surface in the rest of the analysis. The approach described above can be used to determine the reliability index β. Note that the linearization is performed at the design point where the distance from the origin to the failure surface is minimized (Madsen et al 1986). This method of defining and calculating β is referred to as the First Order Reliability Method (FORM) named appropriately for the first order (linear) approximation of the failure surface.

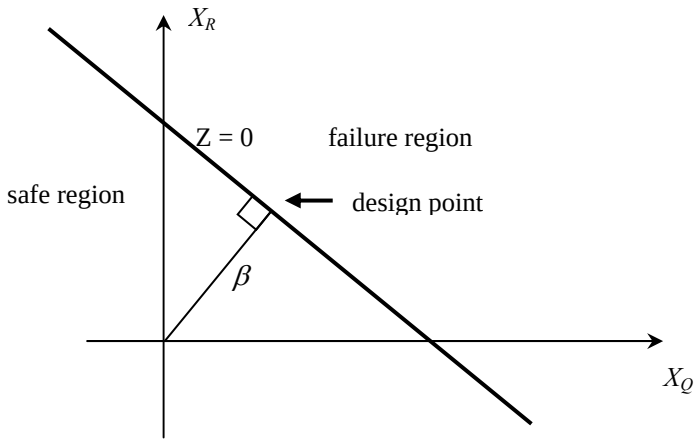

Figure 1-1: General Definition of Reliability Index β in the Standardized U Space

Furthermore, in general situations when the resistance R and load effect Q are not normally distributed, they may be approximated using normal variables. These normal variables are determined such that they have the same probability density values and cumulative probability function values as the original random variables at the design point on the failure surface, where β is then measured as the shortest distance to the origin (Madsen et al 1986). In general, the design point is not known prior to the computation. That is also the point where linearization of the failure surface is to be performed and the non-normal variables to be converted to normal variables and then standardized. Therefore an iterative approach is required to calculate the reliability index β when the random variables involved are not normal variables and/or the failure surface is not linear.

In this research project, FORM is used to assess the safety level of bridge components to evaluate the reliability indices for the superstructure of highway bridges in Michigan. In reality, assuming random variables to be normally distributed may not always be valid for the resistances and load effects involved here. When this is the case, a hand calculation of reliability index β using Equation 1-6 may not be accurate enough. Thus in this study a computer program developed using MATLAB software was used to compute the β values, using the iterative approach discussed above.

1.4 AASHTO LRFD Bridge Design Specifications and Calibrated Safety Level

The AASHTO LRFD Bridge Code (1998) was calibrated using the same concept of bridge structural safety (Nowak 1999). More specifically, the research effort of calibrating this new set of specifications

used the same method of structural reliability index β as briefly presented above in Section 1.3. The target reliability index used (Nowak, 1999) was 3.5. This is approximately equal to two failures in 10,000 (see Table 1.1) It is important to note that failure was defined in Nowak (1999) and in the present study as exceeding some predefined limit state and not necessarily a global collapse. It is also critical to understand that selection of a target reliability index was somewhat arbitrary. In that study, 3.5 was selected to provide the same average safety margin in the LRFD Bridge Code that was estimated to exist in the previous AASHTO bridge design code. Thus, it is appropriate to state that that the particular target value 3.5 reflects an average of safety levels typically practiced in the country over several decades.

This research project uses the same structural reliability concept to assess structural safety of bridges designed using the new AASHTO LRFD resistances. In addition, many statistical parameters including the mean and standard deviation of the involved random variables are consistently used in this research project, so that the target β value of 3.5 can eventually be used as the criterion for calibration of the Michigan design load. In addition, the truck loads used in the reliability analyses in this study were modeled based on weigh-in-motion (WIM) truck weight data gathered at 42 locations throughout the state of Michigan. The details of procurement and processing of the data are discussed later.

1.5 Organization of Report

This report contains seven chapters. Chapter 1 has provided an overview of the research project. This includes background and motivation for this investigation, research objective and scope, and the calculation procedure for the reliability index β. It also offers discussions on the requirement for β as the reliability index for eventually calibrating the load factor in the state of Michigan. Chapter 2 presents a summary of the large WIM data sets used within this study. Chapter 3 presents details regarding the projection of all load effects statistics. This involved 72 load effects for five different functional classifications for a total of 360 different statistical distributions. Significant attention was paid to data processing to cover a weakness with some previous bridge reliability studies. Chapter 4 presents the details of the reliability analysis for assessing the safety of bridges, covering the following four types of common bridge construction in Michigan in recent years. 1.) Steel beam bridges (SC), 2.) Prestessed concrete I beam bridges (PI), 3.) Adjacent prestressed concrete box beam bridges (PCA), and 4.) Spread prestressed box beam bridges (PCS). Chapter 5 covers the calibration for the load factor needed to provide a reliability index of 3.5. Chapter 6 presents a discussion on the impact of potential increases in the load factor for the state of Michigan. Finally, Chapter 7 presents conclusions and recommendations regarding highway bridge design practice in Michigan.

Chapter 2: Procurement and Organization of Bridge and Truck Data

Chapter 1 has indicated the scope of this study covering 20 typical bridges randomly selected from the population of new bridges built in the past 15 years. Table 2-1 lists these 20 bridges, 5 from each of the 4 typical beam types: steel (SC), prestressed I (PI), prestressed concrete adjacent box (PCA), and spread prestressed concrete box (PCS). The table also provides some general information on the structural arrangement including the number of spans, whether the spans are continuous or simple, and span length. The load effects on these bridges, namely shears at moments at critical locations on each bridge, were used to develop a "portfolio" or suite or reliability indices later in this study. It is this suite of reliability indices that provides the means for calibration of the LRFD Bridge Code.

Table 2-1 Bridges used in Reliability Analysis

Bridge Type and I.D.	Number of Spans	Length of Spans (span no.)	Continuous or Simply Supported
SC			
11072-B01	2	66' (1 & 2)	Continuous
19042-S03	4	151' (1), 127'-2" (2 & 3), 152'-6" (4)	Continuous
41064-S20-3	1	130'-7"	Simply Supported
41064-S18	1	146'	Simply Supported
63174-S19	2	145'-3"(1), 160'-10"(2)	Continuous
PI			
19033-S11	1	129'	Simply Supported
11112-B02	7	118'-6"(1 & 7), 116'-3"(2,3, & 6), 116'-9"(4 & 5)	Simply Supported
11052-B02	4	98'(1), 98'-5"(2,3 & 4)	Simply Supported
19034-R01	3	41'(1 & 3), 32-6"(2)	Simply Supported
11057-B04	7	123'-9"(1 & 7), 123'(3,4,5 & 6)	Simply Supported
PCA			
46082-B02	1	41'-4"	Simply Supported
82022-S05	2	71-6"(1 & 2)	Simply Supported
82022-S06	2	71'-6"(1 & 2)	Simply Supported
82022-S25	1	95'-7"	Simply Supported
11015-S01	4	36'-5"(1), 76'-10"(2 & 3), 41'-11"(4)	Simply Supported
PCS			
33084-S14	3	38'-5"(1), 70'-7"(2), 34'-11"(3)	Simply Supported
55011-R01	1	72'-9"	Simply Supported
63081-S06	3	28'(1), 73'-10"(2), 29'(3)	Simply Supported
79031-B01	1	46'-7"	Simply Supported
03072-B04	1	52'	Simply Supported

For the reliability assessment of moment and shear for beams, equation 1-3 above can be expressed as

$$Z = R - D - L \tag{2-1}$$

where $D + L = Q$. D and L are the dead and live load effects, respectively. Live load refers to truck load effect on bridge components such as moment and shear. Both are modeled as random variables in this study. In order to estimate the reliability indices for the twenty bridges it was necessary to calculate the statistical distributions for the live load effect. This chapter discusses the data procurement. The live load effects are truck induced moment and shear for beams.

Five years of truck data were procured from MDOT's Bureau of Transportation Planning, Asset Management Division. The data was organized into five (5) functional classifications (FC) of roadway

prior to influence line analysis. The total number of trucks was approximately 101 million. Table 2-2 presents the truck database size for each FC.

Table 2-2 Weight-in-motion (WIM) Database Description for Principal Arterial

Functional Classification	FC01	FC02	FC11	FC12	FC14
Description	Interstate rural	Other rural	Interstate urban	Other freeway	Other urban
Number of trucks	41,694,600	5,952,000	30,132,000	19,418,500	4,154,000
Total	101,351,100				

These Functional Classifications included 1.) FC01: Principal Arterial – Interstate Rural; 2.) FC02: Principal Arterial – Other – Rural; 3.) FC11: Principal Arterial – Interstate – Urban; 4.) FC12: Principal Arterial – Urban; and 5.) FC14: Other Principal Arterial – Urban. It should be noted that all the data available for use in this project was for principal arterial roadways of some type.

Five bridges of each type were selected from the Michigan Department of Transportation's bridge inventory: steel girder (SC), prestressed concrete I-beams (PI), prestressed concrete spread box girders (PCS), and prestressed concrete adjacent box girders (PCA). All of these bridges are designed with a composite concrete deck. The bridges were selected randomly; however, recall from MDOT Research Report RC-1413 that there was a requirement that the bridges be constructed or re-constructed after 1990. The purpose of this imposition was to ensure that the load factors calculated in this study were done so for bridges that were representative of structures currently being designed in the state of Michigan. Some bridge details, including their locations and number of spans, are shown in Table 2-1. In addition, WIM truck weight data gathered by researchers at the University of Michigan (Nowak et al 1994) are also included in this calibration effort.

Beam flexure and beam shear

Similar to the previous report (van de Lindt et al., 2002), in order to assess the reliability for beam flexure and beam shear it was necessary to numerically run each truck over influence lines for each bridge. Multiple influence lines were checked for each bridge and the maximum moment and shear were computed by combining the truck axle weights in the database and the influence lines. For example, if a two-span continuous steel composite (SC) bridge was being analyzed then it would be necessary to identify the critical positive bending moment on each span, the negative bending moment at the interior support, the shear at each end support, and the shears to the left and right of the center support. Each of these load effects was processed and a reliability index associated with that load effect was computed. This was done using a data processing software package developed specifically for this study.

Chapter 3: Development of Truck Load Statistics

In order to perform the reliability analysis using FORM (see Chapter 1) for the 20 bridges in this study it was necessary to project the live load, i.e. moment and shear as described below. If the live load data was used un-projected it would result in high reliability indices not really representative of the reliability over the bridge's design lifetime. Data projection is a technique commonly employed in reliability analyses and there are many different methods each with their own pros and cons. In NCHRP 368 (Nowak 1999) the live load data projection was done using a graphical technique which may be shown to not be able to be reproduced exactly. This chapter describes the method and results of a systematic procedure to determine which data projection method most accurately reproduced the mean value of the longer-term data set. The MDOT study described in this report is unique in that it involves a large enough data set to provide the short-term statistics, which can be used to check the accuracy of the projection.

3.1 Determining Average Daily Truck Traffic (ADTT)

From the ADTT statistics, the same procedure used in van de Lindt et al. (2002) was used to project the moment and shear data to 75 years. That procedure is as follows:

The equivalent days of data (EDD) for each functional class was determined based on the 50th percentile of the ADTT data for the entire state of Michigan. The 50th percentile means that half the measured ADTT's on roadways in the state of Michigan were below and half were above the value used. Specifically, the EDD was determined as

$$EDD = \frac{m}{ADTT} \tag{3-1}$$

where the numerator is the number of trucks in the dataset for that FC from Table 2-1, and the denominator in equation 3-1 is the ADTT corresponding to the n^{th} percentile from the corresponding planning dataset. It was decided after discussion between the researchers and project manager to use the 50th percentile of the empirical cumulative distribution function (CDF) of the ADTT (from planning) for each FC. The 50th percentile was chosen because it is a well-known representative statistic called the median. The median (50th percentile) is defined as the data point at which one-half of the data is below and one-half of the data is above. These CDF's were calculated by dividing the miles of roadway associated with each truck volume in the planning dataset into one-tenth mile segments. For example, if a particular segment of roadway was two miles long and had a small ADTT and another segment of roadway was one-half mile long but had a large ADTT, the new weighted data set would have twenty data points (2 miles/0.1 mile) with the small ADTT values and five points (0.5 miles/0.1 mile) with the large ADTT values. It was reasoned that the vast majority of bridges in the state of Michigan are less than 0.1 miles in length, i.e. 528 feet, and therefore a roadway segment of this length would, in theory, encompass an entire bridge. All these points would be generated and placed in a data set that makes up the weighted dataset from which the 50th percentile was determined for the projection procedure. This procedure is consistent with Phase I of this study (MDOT Research Report RC – 1413). It should be noted that the discrete WIM locations were not coupled with the ADTT estimation directly. Rather, as described above, the ADTT was related to the miles of roadway in the entire state of Michigan.

The number of days to which the data must be projected, termed the required days of data (RDD), was calculated as

$$\begin{aligned} RDD &= 75 \text{ years} \times 365 \text{ days/year} \\ &= 27,375 \text{ days} \end{aligned} \tag{3-2}$$

where the right hand side of equation 3-2 is the number of days in 75 years.

3.2 Projection Models

3.2.1 A general procedure

Survey data for the load effect (moment or shear), represented by the random variable x can be represented using an empirical or parametric statistical distribution function. This function could be given in the form of probability density function (PDF), $f(x)$ or cumulative distribution function (CDF), $F(x)$. When the maximum value of the random variable over an *n*-year period is of interest, we may first establish the relationship between *N*, the number of occurrences of the random event, with the future time period *t*,

$$N = g(t) \tag{3-3}$$

The function $g(t)$ can be estimated using the WIM data previously discussed in Chapter 2. The corresponding CDF model for the maximum value of the random variable x at a future time period t , i.e. 75 years, can be written as

$$F_{\max(t)}(x) = F(x)^{g(t)} \tag{3-4}$$

Note that $F(x)$ is a distribution model for data collected over a relatively short time period, for example, several days. While $F_{\max(t)}(x)$ is typically a distribution model for the maximum value of that data in a longer (or much longer) period, say, in years. Thus equation (3-4) indicates projection from a short period to the longer one for the random variable x (in our case moment or shear). The PDF of the long term maximum could be found by taking the derivative of equation (3-4) with respect to x,

$$f_{\max(t)}(x) = \frac{dF_{\max(t)}(x)}{dx} = g(t)F(x)^{g(t)-1} f(x) \tag{3-5}$$

If the PDF of the maximum value is known, one can readily estimate the mean, standard deviation, and higher statistical moments (e.g. variance) of the maximum value using basic statistical methods. If the PDF of the maximum value in (3-5) is analytically intractable, numerical integration may be applied. One should note that the statistical moments (i.e. mean and variance) of the maximum value are functions of time *t* only.

3.2.2 A practical method

A practical approximation of the expected maximum value over an *n*-year period that is sometimes adopted by (research) engineers provides a more straightforward solution. This type of method was used approximately (heuristically with a curve instead of a line) by Nowak (1993, 1999) to develop a vehicle load model for the calibration of the AASHTO LRFD bridge design code. The approximation can be calculated as,

$$E[x_{\max(t)}] = F^{-1}\left(1 - \frac{1}{g(t)}\right) \tag{3-6}$$

where $E[x_{\max(t)}]$ is the expected value of the maximum over time *t*.

Note that the general procedure in equation (3-5) above yields the expected maximum as,

$$E[x_{\max(t)}] = \int_{-\infty}^{+\infty} x f_{\max(t)}(x)dx = \int_{-\infty}^{+\infty} x g(t)F(x)^{g(t)-1} f(x)dx \tag{3-7}$$

The expected maximum values computed from equation (3-6) and (3-7) will be very close when $g(t)$ is a large value, which is usually true for most practical predictions. The assumption is made that the value

corresponding to a certain probability percentile is the same as the expected value of the maximum. It should be noted that this assumption can be biased when $g(t)$ is small, say, two. The expectation of the maximum of two data points independently drawn from a single distribution, say, the standard normal distribution, should be greater than 0, which is the estimation of the $E[x_{\max(t)}]$ from equation (3-6). But this approximation can still be used when $g(t)$ is large enough and the desired accuracy level is not unreasonable. Another drawback of this approximation is that it does not provide the higher order statistical moments of the maximum value distribution that may be needed (such as the variance of the maximum needed in reliability analysis).

3.3 Models for Short-term Data

The projection procedures discussed above are independent of the statistical models ($F(x)$ in equation (3-4)) representing the distribution for the underlying random variable. However, an accurate model is, of course, another important element for accurate projections. The models can vary significantly depending on the relationship between the data set and the physical phenomena or process. This means that there is no universal model appropriate for all data. In fact, a model that performs poor in representing one data set might perform well for a different data set. In the present case we are interested in representing the WIM load effect data sets as accurately as possible.

3.3.1 Global linear regression model

This model has been used extensively in civil engineering applications (see e.g. Ditlevsen, 1988; Nowak, 1993). Initially, the data needs to be sorted in ascending order and each is assigned an empirical CDF value. The value for the n^{th} data point x_n is written as

$$F_{empirical}(x_n) = \frac{n}{N+1} \tag{3-8}$$

where N is the total number of data points. Then, probability paper (see e.g. Ayyub and McCuen, 1997) for the desired statistical distribution can be used to plot the data points against the empirical CDF values. Finally, linear regression using all the points on the probability paper is performed to find the statistical parameters of the distribution. The suitability of such a linear regression model depends significantly on the probability paper selected and its corresponding parametric statistical model. The normal distribution is used most often in engineering practice for this purpose, often due to incomplete information about the physical process being modeled.

An example of global linear regression using a normal distribution model for the mid-span bending moment on a simply supported bridge (Bridge ID 33084-S14, 1st Span) 38.4 ft in length is shown in Figure 3-1. The data presented was collected over a two-day period. One can see that the model fits most of the data points in the middle but significant discrepancies are apparent in the tails of the distribution. By applying the aforementioned projection method, the $F(x)^{g(t)-1}$ term becomes small very quickly for small $F(x)$ values, say, values smaller than 0.95, when $g(t)$ is a large number. This means that only the part of the model corresponding to large CDF values (right upper tail in Figure 3-1) will have an influence on the projection result. Thus, when the upper tail fits the data poorly, the upper portion of the linear regression will be unrealistic. So will be the projected maximum value of the CDF based on this poor fit will be equally unrealistic.

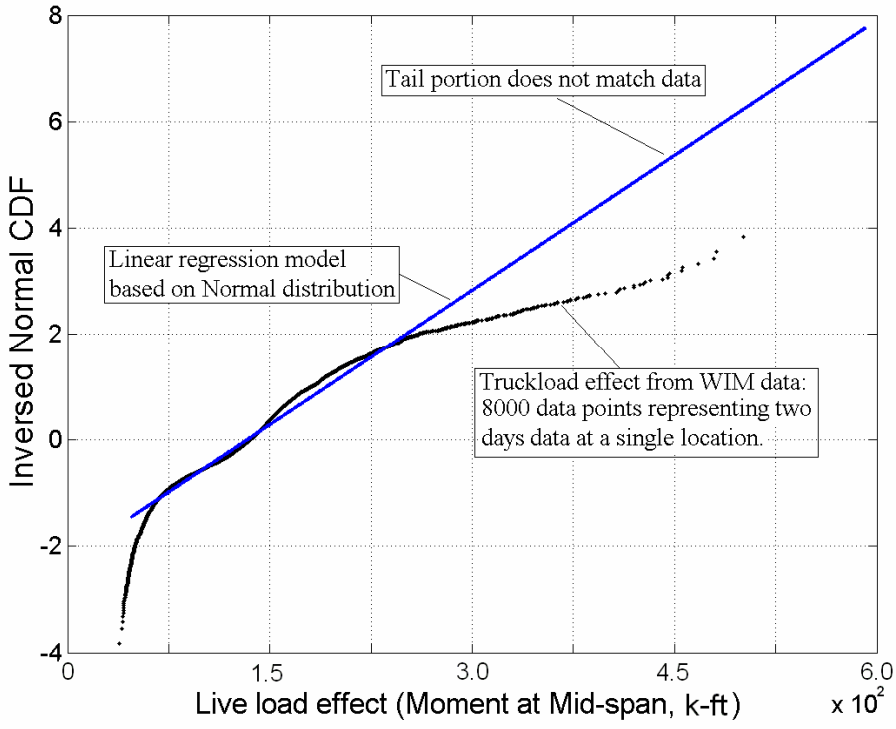

Figure 3-1 Linear regression model of two-day load effect data

3.3.2 Tail-portion linear regression model

Many researchers have stressed the importance of good fitting in the tail portion of the data in future maximum value prediction (e.g. Lind and Hong, 1992; Caers and Maes, 1998). If the distribution model fits short-term data poorly in the tail, projections based on this model will not be reliable because the model fails to describe the part of data that has the most influence on the projection results. This situation together with the 'tail dependence' property of the maximum projection, which will be discussed in detail later, provides an option to construct projection models in which the tail portion of the empirical CDF is treated separately and with significant emphasis. A linear regression model for just the tail-portion may be the easiest and most straight forward way to apply this modeling procedure. First, one need only decide what critical CDF value, denoted as F_c, defines the tail portion of the distribution. Then the data points having empirical CDF values greater than that critical value are used for the linear regression. This approach may result in model parameters quite different from those previously determined when performing a global linear regression using all the available data. The tail regression model applied to the same data set used in Figure 3-1 is presented in Figure 3-2, but using a critical CDF value of F_c=0.98. It is evident that the tail regression model represents the data better than the global linear regression model in the tail region, beyond the critical CDF value.

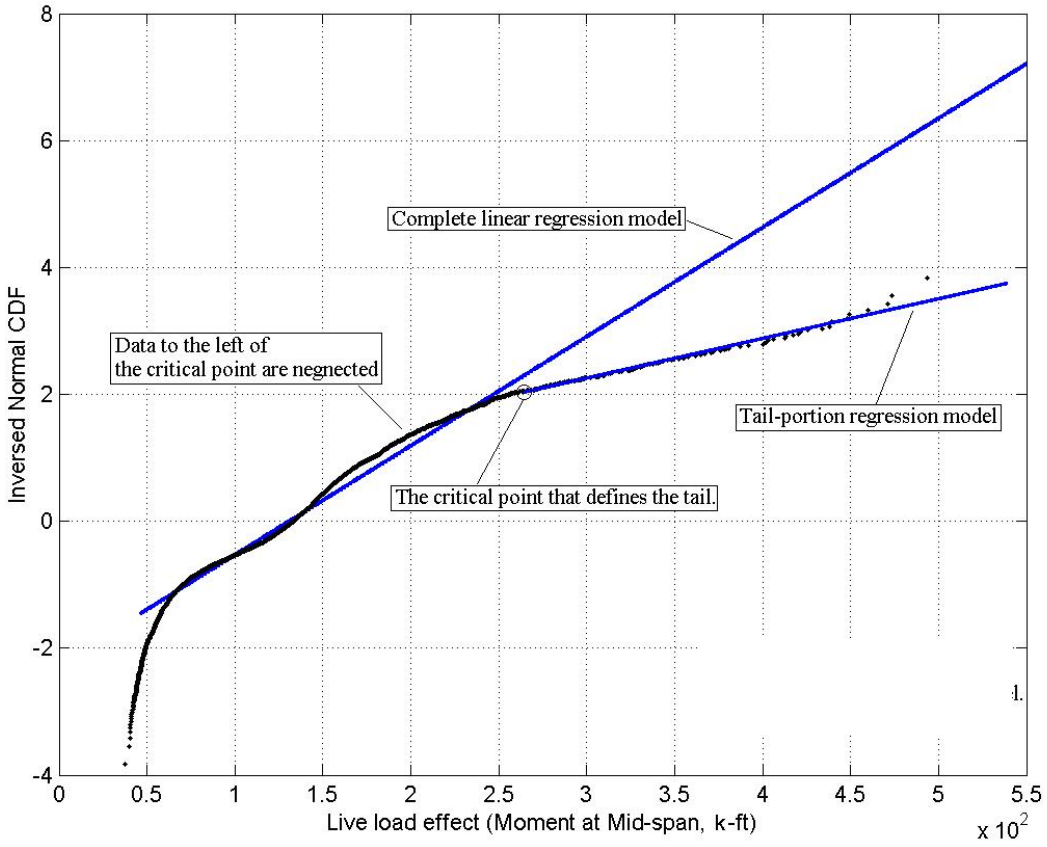

Figure 3-2 Tail-portion linear regression model of two-day load effect data

3.3.3 Tail-portion polynomial regression model

Linear regression models assume that the data follows a linear pattern thus limiting the flexibility of the model. When there is a significant curvature in the tail, this model will not perform satisfactorily. One solution to this is to increase the degrees of freedom associated with the model by using a polynomial regression instead of a linear regression. This polynomial formulation can also be used to perform the normal transformation (Chen and Tung 2003) and simulation (Hong and Lind 1996).

For illustrative purposes, consider the Gumbel distribution model for the data in Figure 3.3, which has a curved tail portion on a standard linear Gumbel probability paper. One can write the linear formulation of Gumbel distribution CDF as,

$$F(x) = \exp(-\exp(h(x))) \tag{3-9}$$

where $h(x) = -a(x-b) \quad a > 0$.

To model the curvature of the tail, replace the linear $h(x)$ with a polynomial from polynomial regression using the data points in the tail region for a better fit of the tail. However, $F(x)$ will still have the properties of CDF as long as the function $h(x)$ is a monotonically decreasing function of x. So the new CDF can be written simply as

$$F(x) = \exp\left(-\exp\left(\sum_{i=0}^{m} a_i x^i \right) \right) \tag{3-10}$$

Let's consider a third order model for illustration by setting m=3:

$$F(x) = \exp(-\exp(a_0 + a_1 x + a_2 x^2 + a_3 x^3)) \tag{3-11}$$

Because of the required monotonically decreasing property of $h(x)$, the coefficients a_i (i=1,2,3) must have the relationship:

$$a_1 < 0, \quad a_3 < 0, \quad a_2^2 < 3a_1 a_3 \tag{3-12}$$

Now, one can perform a polynomial regression within the tail portion to determine the model parameters. It is important to note that this model provides a good fit only in the tail portion. But, as previously shown, the relative error of maximum mean and standard deviation for temporal data projection are bounded. Polynomials higher than third order can also be used, but the models must be checked carefully to make sure that the derived CDF remains monotonically increasing with respect to x. Figure 3-3 presents fitting using several different orders of polynomials for the same truckload effect data previously used to get Figures 3-1 and 3-2.

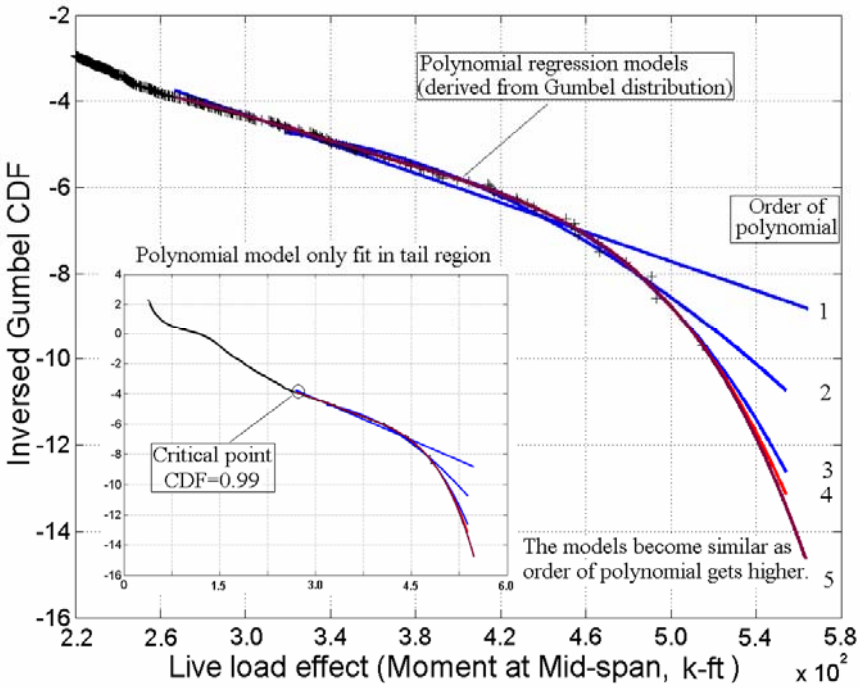

Figure 3-3 Polynomial regression models of different order

A question that naturally arises for this kind of model is what will happen if other distributions, such as the normal distribution, are used to derive this polynomial model? How will the order of the polynomial influence the projected results? To illustrate these influences, twenty different models are constructed based on a two-day truckload effect data set selected at random from the Phase II data. Since the number of days of data is only of relative importance, i.e. to the number of days of data it is being projected to, an ADTT of 5,000 was assumed here. Thus, two days of data is assumed to be represented by 10,000 trucks (and subsequently their load effects) from the large data set provided by MDOT. Four distribution types are used here: normal, Gumbel, lognormal and Weibull distributions. Five models for each distribution type are included with the order of polynomial varied from the first (linear) order to the fifth order. Then,

each model is used to project the set of 10,000 un-projected load effects (from trucks) to the statistical distribution of the maximum load effect for a longer time period. Note that the un-projected 10,000 load effects discussed here could be either moment or shear but is moment in this case. The results of the expected maximum values were listed in Appendix A, Table A-1 (also see Figure 3-4). From the results one can see that the difference between models becomes negligible when the order of polynomial is higher than the third order. This result is not surprising since the effect of the polynomial regression is to adjust the trend of distributions so that they all fit the data in the critical tail area. So if the curvature in the tail is accurately represented by the data points, one could achieve reasonably good projection results using this approach no matter which distribution was used to construct the polynomial model.

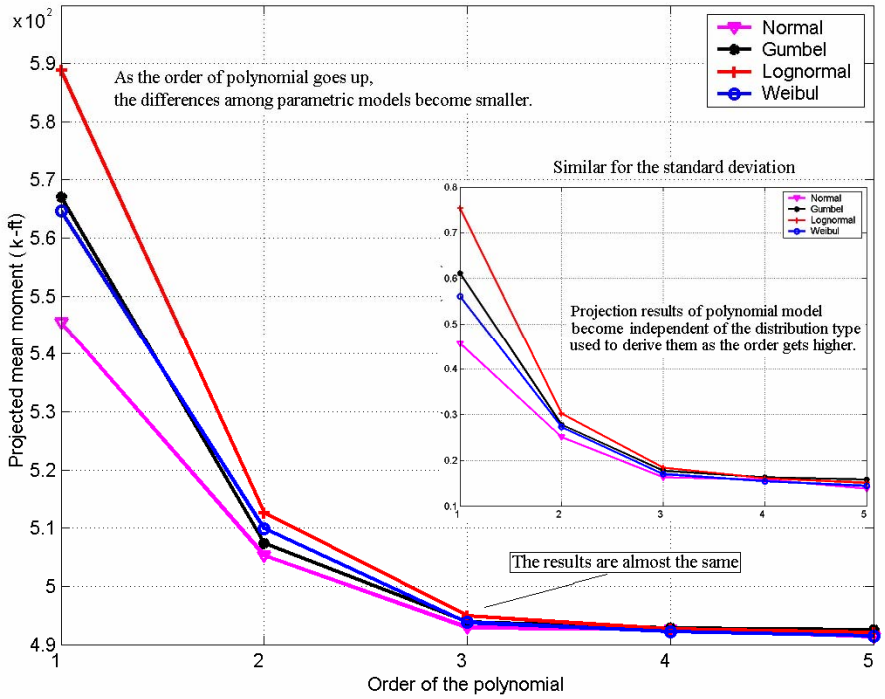

Figure 3-4 Projection results of different polynomial models (Units for both mean and standard deviation are k-ft)

The polynomial regression model can be applied to data that have a curved tail regardless of the probability paper selected. However, it should be noted that a curved tail alone does not necessarily justify the use of this model. In many cases, the curved tail may only be the result of low data resolution in the tail of the data or the presence of several outliers. A situation that is suitable for this model is data with an unknown upper bound as presented in Figure 3-5, which shows a computer generated dataset that follows a normal distribution but has an upper bound of 1,000. The most obvious impact the upper bound has on the tail portion is that the tail turns from a straight line into a curve that eventually becomes perpendicular to the abscissa at the bound value 1000. In reality, the upper bound of the random variable may not be quite as rigid as in this simulated data set. Nevertheless, the polynomial regression model can still track the changing tendency of the CDF in the tail portion without any knowledge of the exact value of the upper bound.

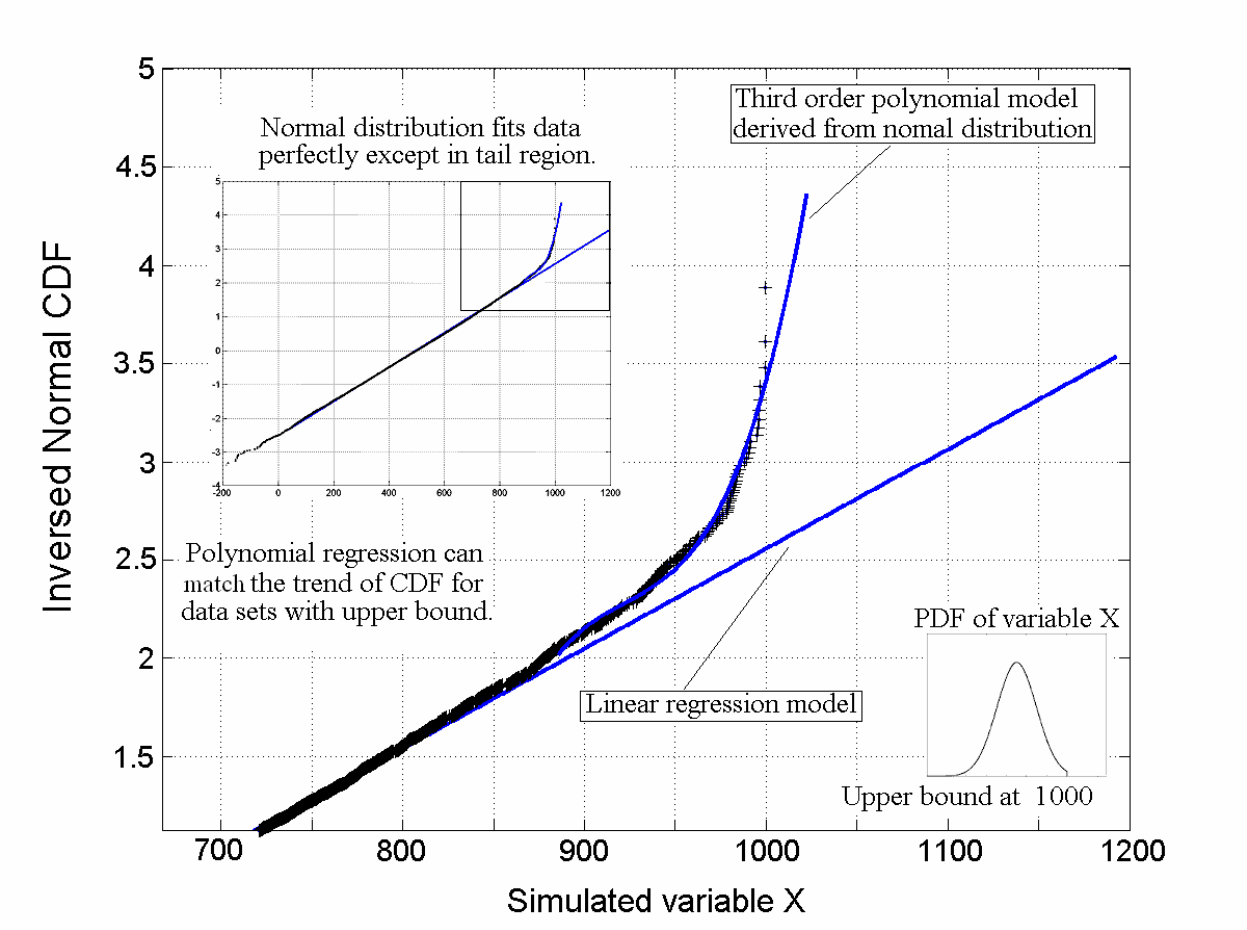

Figure 3-5 Normal distribution with upper bound

3.4 Projection of Bridge Live Load Effects

The weigh-in-motion (WIM) technique is a field survey method used widely in the U.S. highway system to collect truck weight information. This type of data is becoming more accurate and widespread in all 50 states in the U.S. The "short-term" data set used here is the WIM truck record from 42 stations in the state of Michigan arterial highway system, i.e. trunkline roadways, described in Chapter 2. This data set contains axle weights and spacing for all trucks passing 42 WIM locations from 1997 to 2000, and 2003. Additional details and breakdown for this data set were presented previously in Table 2-2. The load effect data was generated using basic influence line techniques, with each data point representing the maximum moment at the mid-span of an 38.4 ft simply supported bridge as a truck is numerically run across the structure. Among all five functional classifications, FC01, FC11 and FC12 data sets were selected for use in this portion of the study because they contain the most truck records and thus have higher accuracy in representing the statistical characters of the load effect. The purpose of following projection evaluations is to find out how each projection model performs in predicting the mean and standard deviation of the maximum load effect in a longer period based on data from only a short period of time.

3.4.1 Numerical experiment design

The large size of the WIM data set provided a unique opportunity to design a test, or experiment, that could evaluate the accuracy and stability of the projection models presented herein. An option was to use part of the data set and project it to get the expected value of the maximum of the entire data set. Then the

maximum value from the entire data set could be used to make the comparison. However, this is not the most reasonable way to make use of such a large data set because the single maximum value of the entire data set itself is not a good representation for the expected maximum value of the data set. Instead, this computed maximum is just a sample, or single value, of the statistical distribution of the maximum and not its mean value. In addition, the higher order statistical moments of the maximum value, e.g. variance, cannot be examined. Almost all engineering applications require that a temporal projection at least provide information for both the mean and variance of the random variable. This is definitely the case for reliability of bridges in the present study.

In this study, another test procedure is designed to verify the projected results. A maximum data set consisting of maximum values was constructed by taking the maximum values from 10 six-month data sets. These six-month data sets came from arbitrarily dividing the five-year data set into ten parts. This maximum data set represents the statistical distribution of the six month maximum (live) load effect for flexural moment in the 38.4 ft example span. With ten data points in it, the mean and standard deviation (standard deviation is used instead of variance for engineering conventions) of the maximum value could be calculated with higher accuracy. These values were used as target values in comparison to the projected values. The mean and standard deviation of the six month maximum load effect for functional classifications 01, 11 and 12 are listed in Appendix A, Table A-2. With the maximum value data set equivalent to a six-month period, a significantly smaller data set, i.e. over a shorter time period, should be used to check the accuracy of the models. So each six-month database was further split into 12 sections representing load effects of shorter period (approximately 15 days) each. Then, these smaller data sets were projected to find the mean and standard deviation of six-month maximum with each of the projection models. This procedure will be explained graphically in Figure 3-6.

Three variations of the model will be investigated here including global regression, tail-portion linear regression, and tail-portion polynomial regression discussed earlier. Each of these will be combined with each of four common parametric models, namely normal, Gumbel, lognormal and the Weibull distribution. Thus, there are a total of 12 projection models presented and compared. Each of these projections is numerically performed based on the general procedure described by equation (3-5), with $g(t)$ equal to a constant representing the total number of trucks in 6 months established from the data.

For modeling convenience, the critical CDF value that defines the tail is arbitrarily set to 0.99 for the tail regression models. A third order polynomial is used in all polynomial models. As a comparison, the projection based on the practical method described in equation (3-6) using the normal distribution is also applied to the same data sets.

The results of the data projections are listed in Appendix A, Tables A-3, A-4, and A-5 for FC01, FC11 and FC12 respectively. Note that the projected mean and standard deviation were normalized by dividing them by the corresponding maximum values calculated from the data, i.e. in Table A-2, which were felt to be reasonably accurate estimations of these statistics. Hence, the closer to unity the values in Tables B-3, B-4, and B-5 are, the more accurate the corresponding model is. The stability of model performance could be examined by comparing the results from the different six-month data sets (No.1 to 10). If these results are close to each other, it means that the randomness from the data set does not significantly effect the performance of the projection model. The test procedure just described can be summarized in following steps (see the flow chart in Figure 3-6):

1. The five-year data set of each functional class is divided into 10 data sets, denoted as subsets No.1 to 10. Each represents a six-month data set. The maximum values for these subsets are found to construct the “maximum load effect data set”.
2. Calculate target maximum load effect statistics from the “maximum load effect data set” in step 1.
3. Each six-month data set is divided into 12 smaller data sets. These small data sets could be regarded

as the "short-term" data set that has been observed, or recorded.

4. Use the small data sets to project to obtain the statistics of six-month maximum load effect. So each six-month data set could provide 12 groups of projection results, with mean and standard deviation in each group. The average value of these results can be used to represent the average level of accuracy of the projection model used. And these average values are normalized with the target values.
5. Repeat step 3 and 4 for every projection model examined. There are 13 of them.
6. Repeat step 3 to 5 for every six-month data set (No.1 to 10).

All of the normalized results (from step 4) are listed in the tables. So each row of the table represents average results from one six-month data set. And the "average" row of the table could be regarded as the overall accuracy indicator of the models over the entire five-year data set.

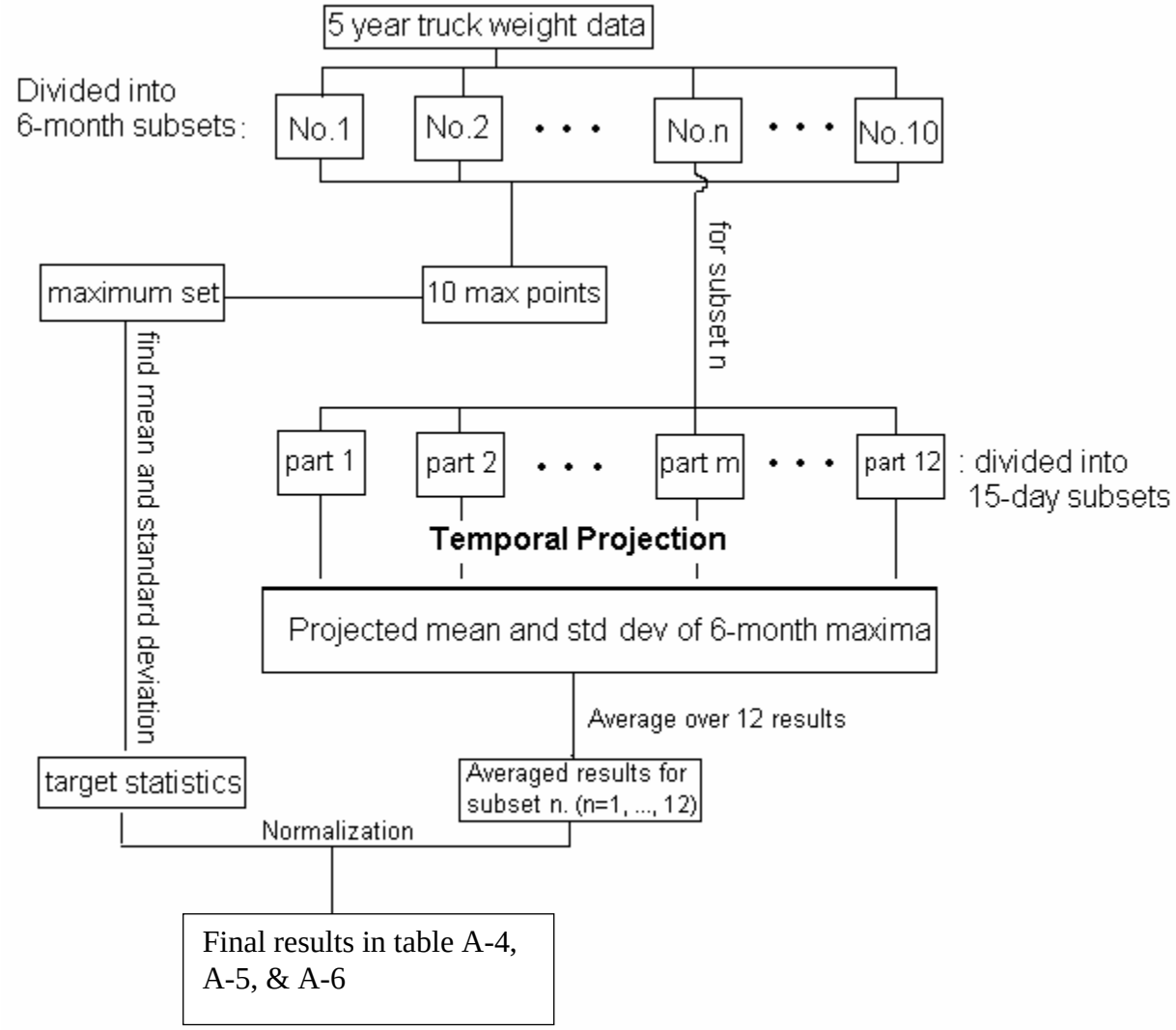

Figure 3-6. Flow chart for numerical experiment

3.4.2 Evaluation of the Models

From Appendix A one can see that the results show no significant dependence on the functional classes, at least for this large data set. A projection model that performs well for one functional class will do well for another. However, some differences between the models are seen here:

Estimation of the mean value

Practical method: The practical method is applied to a linear normal model in this report. Therefore, the results from the practical method are close to those from the linear normal model with the general projection method. The standard deviations listed in the "practical method" column are calculated from a method consistent with that used by Nowak (1993, 1999).

Linear models: The complete linear regression models behave differently according to the pre-selected statistical distribution. The projected mean ranges from 49% (normal model) to 216% (lognormal model) of the actual value. The Gumbel model gives the best estimation of the expected maximum value with a relative error of no more than 15%. However, all the linear models are stable with respect to ten different data sets here, which means that one could expect very close results no matter which part of a large data base is used in the temporal projection.

Tail-linear models: By concentrating on the tail portion, the accuracy of all models is improved except the Gumbel model when compared to the complete regression method. It was also observed that the stability of the models does not change significantly. Most projections based on tail-portion linear models give expected values slightly lower than the value indicated by the data.

Polynomial models: Almost all polynomial models covered in this report show greater variance in their projected results than the linear models. For example, some projected values in table B-3 (polynomial Gumbel projection for subset No.3) is about 100% higher than the target value. Although the overall average results are not far from unity, the stability of these models is not satisfactory.

Estimation of the standard deviation

All models: The projected standard deviations from all models are not satisfactory. Most of the models underestimate the standard deviation significantly. Although some polynomial models give normalized value close to unity, they are quite unstable and do not consistently provide good results. Thus, we can conclude that models that give practically acceptable estimation of the maximum mean do not necessarily guarantee accurate estimation of maximum variance within a similar range.

Reason for the standard deviation projection inaccuracy: It is important to note that the models in this report can only catch the "average tendency" coming from the regression analysis. So part of the randomness inherent in the data (inherent randomness that could not be parametrically modeled.) is missing from the models.

3.4.3 Model with best fit

Based on the numerical experiment presented in this chapter, it can be concluded that for the MDOT statewide WIM data base, the theoretically best projection method is the global Gumbel model. It was decided through discussions between the researchers and advisory panel to use this projection method for thePhase II study. However, although this method may be theoretically most accurate its application within this project was not felt to be possible following discussions between the researchers and MDOT Research Advisory Panel. This is explained in Chapter 4 of this report.

Chapter 4: Reliability Analysis Using LRFD Resistances

In order to calculate the reliability indices provided by the AASHTO LRFD Bridge Code it was necessary to develop statistical distributions for the live load and dead load.

In order to better understand the effect of the data projection method used, we return to a well-known data set. The data set, termed "Ontario data" in Chapter 5 of this report is projected using the Gumbel method. The Phase II data was also projected using the Gumbel method. The results for these projections for the mid-span moment and shear at the support for a 118.5 ft simply supported bridge are presented in Table 4-1.

Table 4-1: Projected reliability indices for mid-span moment and shear at the support for a 118.5 ft simply supported bridge

data	model	Moment					Shear				
		FC14	FC02	FC11	FC01	FC12	FC14	FC02	FC11	FC01	FC12
Ontario	Gumbel	1.99	1.91	1.70	1.77	1.87	-0.79	-0.85	-1.01	-0.97	-0.88
Phase II	Gumbel	4.24	4.05	4.12	4.27	4.30	1.02	0.88	0.93	1.04	1.07

These moment and shear projections are for bridge B02-1112 which is a prestressed I-girder bridge. Moving our attention to NCHRP Report 368, Figure F-7 on page F-13 of that report shows the reliability indices for simple span moments and Figure F-10 on page F-15 shows reliability indices for simple span shears hover around 3.5 Table 4-1 above shows reliability indices for this same bridge average approximately 1.85 for moment and -0.8 for shear. It can be concluded that the Gumbel projection method in Phase II is not consistent with the projection method used in the calibration of the AASHTO LRFD code, i.e. NCHRP 368. Thus, it is not justifiable to use the same target reliability index of 3.5 if a different projection method is used, regardless of whether or not the projection method is accurate.

A target reliability index of 3.5 is a well accepted safety margin for bridge structures, therefore it is not recommended to change this value. Instead it is recommended to use the Phase I projection method with the large Phase II data set in order to develop a Michigan-specific live load factor for LRFD. The Phase I method, although empirical, can be shown to be more consistent with the heuristic approach used in NCHRP 368.

4.1 Live Loads

The live load effects were projected using a theoretical approach (see equation 3-4 for details). Although the Gumbel method was shown to be theoretically more accurate, it does not account fully for physical upper limits on load effect and is not fully consistent with the approach used by Nowak (1993, 1999). The statistical distributions for the maximum moments and shears for the entire state using the Gumbel approach are presented in Appendix B. The Phase I method will be shown to be more appropriate later in this report, and those projected moments and shears are shown in Appendix C. An impact factor of 1.3 was used for all bridges in this study, which is consistent with Nowak (1999). The single lane girder distribution factor (GDF) was calculated according to AASHTO LRFD bridge code and varied depending on bridge type, girder spacing, etc. This single lane GDF was used because the WIM data resolution was not high enough to determine if two trucks could be side-by-side on a bridge or on the bridge at the same time. A bias factor of 0.9 was applied to the GDF for determination of the load effect during reliability analysis. Note that assuming one lane occupation actually underestimates the load effects in these bridge

components. This is because multiple trucks in adjacent lanes on a bridge will, on average, produce a higher load effect. Thus, this may result in slightly overestimated structural reliability index β values.

4.2 Dead Loads

The dead loads were calculated from the bridge plans provided by the Michigan DOT. The dead load was assumed to act as a uniformly distributed load. The critical beam was assumed to be the girder adjacent to the fascia girder, i.e. first interior girder. Any loads that were the result of safety railing, safety barriers, etc. located on the edge were assumed to be distributed to the critical beam with a one-third factor. A 25 psf future wearing surface was included in the dead load for the reliability analysis. The calculated dead load for each bridge is presented in Appendix D and is also available in MDOT Research Report RC-1413.

Recall that each dead load has an associated bias and coefficient of variation (COV). The COV is defined as the ratio of the standard deviation to the mean value. The dead load bias, D_{bias} , can be expressed in terms of the nominal dead load, D_n, and mean dead load, D_{mean}, as

$$D_{bias} = \frac{D_{mean}}{D_n} \tag{4-1}$$

The bias and COV for the dead load were 1.0 and 0.1, respectively which is consistent with Nowak (1999).

4.3 Bridge Capacity/Resistance Calculations

The bridge component capacity or resistance R defined in Eq.2-1 is modeled here also as a random variable. For the 20 sample bridges, the resistances' standard deviations are taken from NCHRP Report 368 to be consistent. In addition, the mean values of these resistances are estimated as the product of their nominal value and a bias factor. The latter are also taken from NCHRP Report 368 (Steel bias = 1.12; Prestressed bias = 1.05) and the former is computed according to the AASHTO LRFD Bridge Design Specifications (2004). The nominal resistance can be computed as

$$R_n = 1.25D + 1.75\left(L + I\right)GDF_n \tag{4-2}$$

Where D is the dead load effect in the concerned member, L is the live load effect, and I is the impact factor. The nominal girder distribution factor for live load calculated according to the LRFD Bridge Code is notated as GDF_n.

The main differences between the AASHTO LRFD and the standard specifications (AASHTO, 1996) include those with respect to: design vehicle load (HS vs. HL93), load factors, distribution factors, impact factors, and skew factors. Note that these 20 sample bridges provided parameters regarding general geometry of the bridges, such as span length, bridge width, number of lanes, beam spacings, etc. The resulting nominal resistances are shown in Appendix E.

4.4 Reliability Calculation

The reliability index is a measure of the reserve capacity in a structural system. The First Order Reliability Method (FORM) was used to calculate the reliability indices in this study (see Chapter 1: Introduction). The shears and moments were calculated at the points along the span(s) corresponding to

the locations that the live load statistics were calculated, i.e. identified as critical locations. All values of bias were consistent with MDOT Research Report RC-1413.

As mentioned previously, the First Order Reliability Method was used to compute the reliability indices in this study. The results are presented in Appendix G for the WIM load data collected in the metropolitan Detroit area (Nowak et al 1994) and projected to 75 years using the Phase I projection method, see Appendix F. Note that the FC02 column has been omitted in Appendix G. This is because the amount of this FC present in Region 7 is extremely small, i.e. several miles of roadway total. Recall that a target reliability index of 3.5, which is the value used in the AASHTO LRFD Bridge Code calibration, was selected for load factor calibration. Inspection of the reliability indices shown in Appendix G for the Metro Region shows that a significant number of these beta values are below the target level. This is believed to be mainly due to heavy truck loads observed in the metropolitan Detroit area. An effective approach to mitigate this situation is to increase the design load requirement so that the bridge capacity will be increased to maintain a level of safety margin (reliability index) consistent with the rest of the state.

Appendix H shows the beta values for the truck loads collected from WIM stations over the entire state and projected to 75 years using the Phase I method, see Appendix C for projected load effect values. It is seen that the lowest beta value is close 4. They all exceed the 3.5 target level, and are thus more than adequate.

Chapter 5: Calibration of Michigan-Specific LRFD Bridge Code Live Load

The objective of this project is to understand what load factor for the HL93 design load can provide Michigan's trunkline bridges with a consistent reliability index of 3.5 using a calibration approach as consistent as possible with that used for the AASHTO LRFD Bridge Code. Mathematically, this can be expressed as the live load factor, γ_L , that provides a reliability index, β, of 3.5.

This is determined by beginning with the LRFD equation for design requirement

$$\gamma_{CD} \cdot CD + \gamma_{WD} \cdot WD + \gamma_L \cdot (LL + I) < \phi \cdot R \qquad (5\text{-}1)$$

where γ_{CD} and γ_{WD} are the dead load factors, CD is the dead load effect, WD is the dead load effect from future surfacing, L is the live load effect, I is the dynamic impact factor, and ϕ is the resistance factor given in Table 5-1.

Table 5-1 Resistance Factors used in Analysis (Nowak, 1999)

Structure Type	Load Effect Type	Resistance Factor, Φ
Composite Steel	Moment	1.00
	Shear	1.00
Prestressed Concrete	Moment	1.00
	Shear	0.90

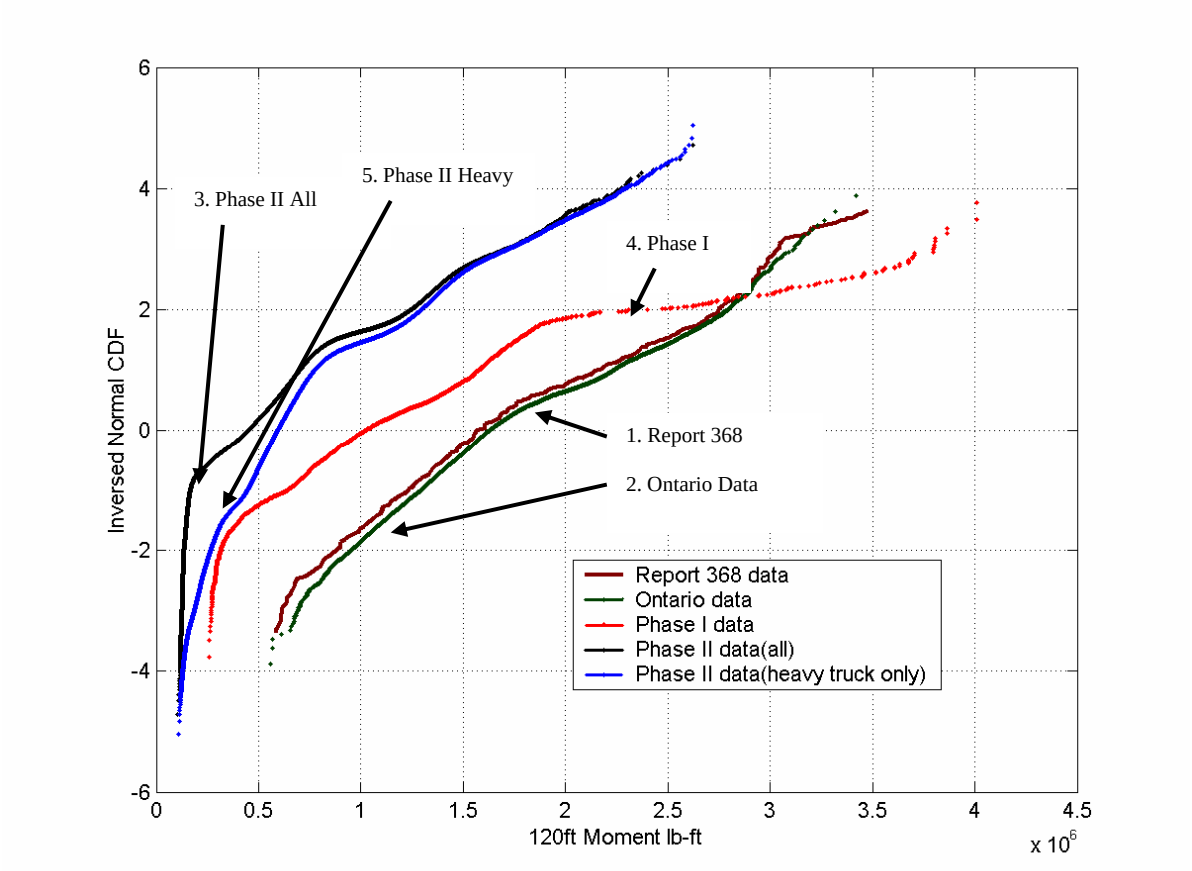

Figure 5-1: Inverse normal CDF for moment at the center of a 120 ft bridge generated using different data sets

Figure 5-1 presents the inverse normal CDF for datasets used in the past and the present study. For illustrative purposes, only the moment at the center span of a 120 ft simply supported bridge is shown in Figure 5-1. The data sets are described as follows:

1. ***Data set 1:*** The plot for the mid-span moment on a 120-ft simply supported bridge from the NCHRP 368 Report was scanned in and digitized. The resulting data will be referred to as "Report 368 data". Note that since the data in the NCHRP 368 report was normalized by the HS20 moment, this normalization was removed by multiplying each value obtained by the HS20 moment.

2. ***Data set 2:*** This data set was acquired from the author of NCHRP 368. This was believed to be the data used for the calculations in the report, but the researchers were not sure. To check this, the recorded trucks in that data set were numerically run over a 120-ft simply supported bridge span and the induced moments at mid-span were recorded. The resulting moment data set is referred to as "Ontario data" hereafter because it was gathered in the Canadian province of Ontario. For further verification, the three Ontario trucks having the largest gross vehicle weight (GVW) were numerically run through the influence line program and it was determined that these trucks produce load effects at least as severe as the HL93. Thus, it can be inferred that these may, on average, produce higher load effects.

3. ***Data set 3:*** The above two data sets are compared with a third mid-span moment data set for a 118.5-ft simply supported span (state bridge ID B02-11112), induced by the recorded trucks used in the current project phase. This data set was acquired by the researchers from MDOT's planning division. This data set is referred to as "Phase II data (all)" and consisted of all recorded truck data available to the researchers. It was made available from Task 4, and was felt to be close enough to the 120-ft span's moment data in the two previous data sets for comparison. Running all Phase II data trucks (101 million of them) over a 120-ft bridge span was considered too time-consuming for the slight difference in bending moment and thus not done.

4. ***Data set 4:*** The Phase I data set as it was used in MDOT Research Report RC-1413. This will be referred to as "Phase I Data".

5. ***Data set 5:*** This data is the same as data set 3, except it was processed in a manner consistent with NCHRP 368. This meant that trucks with two axles having a gross vehicle weight (GVW) less that 10 kips were removed from the data set. In addition, trucks with three or more axles having a GVW less than 15 kips were also removed from the data set. This data set will be referred to as "Phase II data (heavy truck only)".

From inspection of Figure 5-1 it is seen that the data sets 1-Report 368 data and 2-Ontario data are very different from data set 3-Phase II data (all) and data set 5-Phase II data (heavy truck only), as well as data set 4-Phase I Data. Also, it has been pointed out that the upper tail of the data has the most significant effect on the projected 75 year distribution. This means that (1) the Phase II data will have the smallest mean, (2) the Ontario/Report 368 data will have a larger mean, and (3) the Phase I data will have the largest mean value for the projected 75-year maximum distribution. The standard deviations of each data set will not necessarily follow that pattern. If the same projection procedure, regardless of which one, is used to project each data set, the trends described above will be seen.

For consistency of calibration, an approach having more similarity to the concept of Nowak (1999) than the Gumbel projection method is used here to estimate the future statistics of the live load. Accordingly, it is attempted to find a new γ_L in Eq.5-1 to make the beta values close to the target beta of 3.5.

Equivalently, it is to find an additional live load factor in addition to the code prescribed 1.75 to reach the target beta of 3.5.

As a first step, the beta values are calculated using the data sets 4 and 5 (Phase I data set and Phase II data set). The results are given in Appendices G and H, respectively. It has been seen that, for the loads observed in Metro Region, a significant number of beta values are below the target level of 3.5. The average for the values in Appendix G is about 3.1. For other areas in the state, Appendix H shows higher beta values, and the average exceeds 5.0 for all functional classifications of roadway.

An additional load factor is then included to reach a higher average beta values for the Metro Region. See Appendix I for these values. Note that FC02 has been omitted. This is because the amount of this FC present in Region 7 is extremely small, i.e. several miles of roadway total. The additional live load factor used to reach these beta values is 1.2. The average beta value is then raised to about 3.5 from 3.1.

Note also that the calculation approach presented herein underestimates the live load effect because only one lane of the bridge is assumed to be loaded. Equivalently it slightly overestimates the beta values. This calibration result shows that an increase in the live load factor is needed to cover the heavy truck loads observed in the Metro Region, although a further additional amount may be needed to address the overestimation of the beta values.

There are several important issues that were considered during the course of this project and report preparation that warrant some discussion here. The two data sets used in Phase I and Phase II of this study were gathered using two different techniques. In Phase I, strain gages were used in combination with sensors to determine axle spacing and the bridge was essentially used as a scale. In Phase II piezo-sensors located under the pavement were used. The additional live load factor recommendation in this report is based on the Phase I data set, but it should be noted that the same type of data (strain gages on bridge) was not available for the entire state of Michigan. There is not enough information to know which, if any, data set is biased. It should also be mentioned that it is the view of the authors based on current literature that the method used for data collection in Phase I is more reliable than the piezo-sensors used to collect the Phase II data.

Two additional options which were considered were to (1) apply an additional load factor to a particular route, such as I-75 or I-94; and (2) base the additional live load factor on ADTT. The Phase I data used in this study is not only from Interstate routes, thus there is no strong evidence to support basing the load factor in the type of route. In theory, the additional live load factor should depend on ADTT since the probability of having a heavier truck over 75 years increases with increasing volume. The results of a sensitivity study performed using the Phase II data set (the Phase I data set did not have enough data points to perform the same sensitivity analysis) is shown in Table 5-2. This table shows the change in reliability index for the bending moment of a second span (M25) in beige R01-19034, a prestressed I-beam. The results show that ADTT has little influence on the reliability index, if any. This also means that ADTT would have little effect on the required additional live load factor. This is because as the live load factor is increased, the reliability index also increases. Finally, it is important to mention that with regards to both the options considered above, one must consider the fact that although the heavier trucks tend to drive on the same routes, they can, in theory, take any route. However, the probability of the heavier truck, even the heaviest truck over the design life of the bridge, taking this alternate route is very low.

Table 5-2: Beta change with ADTT using Phase II data

ADTT	Beta change %
1000	3.2
3000	2.29
5000	-0.85
7000	-1.705
9000	-2.332
10000	-2.37
20000	-2.556
40000	-2.029
60000	-0.4567
80000	0
100000	0

Chapter 6: Impact of Proposed Bridge Design Load

When the design vehicle load for a jurisdiction is changed, it is expected that the cost of new bridges will change accordingly. This chapter presents our effort to estimate the cost impact for a number of scenarios of increase in the vehicular design load (i.e., live load) for the highway bridges in the Metro Region of MDOT.

The cost impact is quantified here as a multiplicative factor on top of the current cost for the Metro Region as the increment cost. Note that the reference design load (i.e., the current design load) is the AASHTO HS25 load. The increase in the vehicular design load is expressed using an additional live load factor. The cost data in NCHRP Report 495 (Fu et al, 2003) are used here as a reference for the estimation. The additional cost estimation results are shown in Table 6-1.

Table 6-1: Cost Impact of Increasing Design Live Load

Additional Live Load Factor	Cost Impact Ratio
1.1	1.020
1.2	1.045
1.3	1.070
1.4	1.095

In Table 6-1, the first column indicates the possible additional live load factor on top of the live load factor in the AASHTO LRFD Bridge Code (1998). The live load factor and the design vehicular load for strength I, for example, is 1.75 and HL93. Thus the scenarios of total live load for design indicted in the first column are 1.1(1.75)HL93, 1.2(1.75)HL93, 1.3(1.75)HL93, and 1.4(1.75)HL93, respectively. The second column contains corresponding cost increase factor for these scenarios of increased live load factor. Namely, 1.020 means a 2.0% increase, 1.045 means a 4.5% increase, and so on.

A discussion of the details of the estimation process follows. First, the new trunkline bridges constructed in the Metro Region in the past 10 years were identified. This population defines the scope of the cost impact analysis. A total of 77 bridges were identified. These bridges were grouped into 5 groups: steel beams, prestressed concrete I beams, reinforced concrete beams, prestressed concrete adjacent box beams, and prestressed concrete spread box beams. The cost impact analysis was then carried out considering the span length for each bridge. The cost impact ratios for all the bridges in this population were then averaged with weights considering the deck area of each bridge. Table 7-1 shows the weighted averages in the second column for all the scenarios of additional live load factor considered.

NCHRP Report 495 (Fu et al 2003) offers bridge cost impact ratios for the design loads of HS20, HS22.5, and HS25 with regards to bridge type (steel, reinforced concrete, prestressed concrete, etc.) and span length (30ft, 40ft, … 240ft). For this present study, cost ratios with regard to the HL-93 design load are needed. Hence, the scenarios of design load in terms of HL-93 in Table 6-1 were first "converted" to equivalent HS loads in terms of moment. Then interpolation or extrapolation was performed using the data in NCHRP Report 495 (Fu et al 2003) for the cost impact ratios needed here.

After the cost ratios are estimated for each bridge in the metro population, the weighted averaged cost impact ratio for the bridge population was obtained using the following formula.

$$\text{Cost Impact Ratio} = \frac{\sum \text{individual bridge deck area x individual bridge cost impact ratio}}{\sum \text{individual bridge deck area}}$$

The deck areas for the bridges are taken from the Michigan state bridge inventory. The summation is over all the bridges included in the population of those built within 10 years in the Metro Region. The cost increase ratios are taken from NCHRP Report 495 (Fu et al 2003). The formula shows that the "weighting" is done according to the deck area, which is a typical basis for cost estimation at the network level.

Chapter 7: Conclusions and Recommendations

As a result of the analysis in this study, it was determined that some of the projection methods compared in this study, although theoretically correct, are different from the approach used in NCHRP Report 368. The use of the Gumbel tail projection approach, although possibly more accurate, would require a new target reliability level as demonstrated at the beginning of Chapter 4 of this report. The target reliability index of 3.5 used for the AASHTO LRFD Bridge Code is a well accepted safety margin for bridge structures, therefore it is not recommended to change this value. Thus, it was decided to use the Phase I projection method, specifically raising the value of the CDF to the n^{th} power to estimate the statistical distribution of the 75 year load effect. This projection approach is the Phase I method, although empirical, it is as consistent as possible with the approach used in NCHRP 368.

The calibration results show that for the Metro Region, bridge design requires an additional live load factor of 1.2 to provide a reliability index consistent with the rest of the state. This is a result of the heavy truck loads observed in the area. For the rest of the state, this additional factor is not needed. It is recommended to the Michigan Department of Transportation that this additional live load factor be adopted when the LRFD Bridge Code is accepted as the mandatory design specifications.

For the recommended live load increase for the Metro Region, a cost impact of 4.5% was estimated in order to achieve the higher bridge capacity.

References

AASHTO (1998). "LRFD Bridge Design Specifications" 2nd Edition, 1998, Washington, DC

AASHTO (1996). "Standard Specifications for Highway Bridge Design" 16th Ed. 1996, Washington, DC

Benjamin J. R. and C. A. Cornell. "Probability, Statistics, and Decision for Civil Engineers", McGraw-Hill, Inc., 1970.

Chatfield. C. "Model Uncertainty, Data Mining and Statistical Inference", *J.R. Statist. Soc.* A (1995) 158, Part 3, 419-466

Caers. J. and M. A. Maes "Identifying tails, bounds and end-points of random variables", *Structural Safety* 20(1998) 1-23

Chen X. and Tung Y. K. "Investigation of polynomial normal transform", *Structural Safety* 25 (2003) 423–445.

Ditlevsen. O. "Extremes and First Passage Times with Applications In Civil Engineering" dissertation, Technical University of Denmark, Lyngby, Denmark, 1971.

Ditlevsen. O. "Distribution of Extreme Truck Weights", *Structural safety*, 5(1988) 145-148

Fu,G., Feng,J., Dekelbab,W., Moses,F., Cohen,H., Mertz,D., and Thompson,P. "Effect of Truck Weight on Bridge Network Costs", NCHRP Report 495, 2003 Transportation Research Board, National Academy Press, Washington D.C.

Hong H. P. and Lind N. C. "Approximate reliability analysis using normal polynomial and simulation results", *Structural safety* 18(1996) 329-339

Kim, S., Nowak, A.S., and Till, R. (1996). "Verification of Site-Specific Live Loads on Bridges." Proc. 7th ASCE Specialty Conference on Probabilistic Mechanics and Reliability, Worcester, MA.

Leadbetter M.R and Lindgren. G. "Extremes and Related Properties of Random Sequences and processes" Springer Verlag, NewYork, NY, 1983

Lind. N.C and Hong. H.P. "Tail Entropy Approximation", *Structural safety*, 10(1991) 297-306

Madsen, H.O., Krenk, S., and Lind, N.C. (1986). "Methods of Structural Safety." Prentice Hall, Inc. Englewood Cliffs, NJ.

Moses, F. and Verma, D. (1987) "Load Capacity Evaluation of Existing Bridges," NCHRP Report 301, Transportation Research Board, National Academy Press, Washington D.C.

Nowak A.S., Kim, S., Laman, J.A., Saraf, V., and Sokolik, A.F. (1994). "Truck Loads on Selected Bridges in the Detroit Area." Research Report UMCE 94-34, Department of Civil and Environmental Engineering, University of Michigan, Ann Arbor, MI.

Nowak, A.S. (1999) “Calibration of LRFD Bridge Design Code,” NCHRP Report 368, Transportation Research Board, National Academy Press, Washington D.C.

Nowak. A.S. (1993) “Live Load Model for Highway Bridges”, *Structural safety*, 13(1993) 53-66

Perdikaris,P.C. Petrou,M.F., and Wang,A. (1993). “Fatigue Strength and Stiffness of Reinforced Concrete Bridge Decks”, FHWA/OH-93/016, Civil Engineering Dept., Case Western Res. Univ., OH

van de Lindt, J.W. and Fu. G. “Investigation of the Adequacy of Current Bridge Design Loads In the State of Michigan”, Research Report RC-1413, 2002, Michigan Department of Transportation, Lansing, Michigan.

Appendix A: Comparison of Projection Models

Table A-1 Results from polynomial models (Moment 10^5 lb-ft for mean, 10^{10} lb^2-ft^2 for variance)

Polynomial	Maximum in 10000 trucks	Normal	Gumbel	Lognormal	Weibull
1st order model	Mean	5.299	5.509	5.721	5.486
	Variance	0.196	0.352	0.537	0.297
2nd order model	Mean	4.909	4.930	4.980	4.954
	Variance	0.060	0.073	0.086	0.070
3rd order model	Mean	4.789	4.799	4.808	4.797
	Variance	0.025	0.030	0.032	0.027
4th order model	Mean	4.785	4.788	4.786	4.782
	Variance	0.024	0.025	0.025	0.023
5th order model	Mean	4.774	4.785	4.780	4.775
	Variance	0.018	0.024	0.022	0.020

Table A-2 Maximum load effect statistics - flexural moment on a 38.4 ft span (K-ft)

Maximum Data set	No.	FC01	FC11	FC12
Six-month Data sets	1	942.0	630.5	652.0
	2	690.4	533.5	672.2
	3	801.2	505.6	604.4
	4	780.7	529.5	559.0
	5	797.0	621.6	572.4
	6	724.6	899.9	839.3
	7	669.6	822.2	736.4
	8	728.5	755.0	696.7
	9	730.5	800.2	798.0
	10	737.2	608.4	618.0
Maximum Statistics	Mean	760.2	670.6	674.8
	Std. Dev.	73.0	131.6	89.0

Table A-3 Projection test results of FC01 database (Normalized)

FC01	No.	Practical Method [Equation 3-6]	Linear models				Tail-linear models				Polynomial models			
			N*	G	L	W	N	G	L	W	N	G	L	W
Mean Of Max	1	0.49	0.50	0.95	1.83	0.52	0.65	0.79	0.82	0.66	0.93	1.07	0.79	0.93
	2	0.50	0.50	0.95	1.74	0.51	0.66	0.80	0.84	0.67	0.96	1.13	0.87	1.88
	3	0.49	0.49	0.93	1.68	0.50	0.66	0.80	0.83	0.67	1.04	2.08	1.40	1.09
	4	0.47	0.48	0.88	1.35	0.46	0.64	0.77	0.80	0.64	0.99	1.27	0.90	1.02
	5	0.49	0.49	0.94	1.85	0.51	0.64	0.77	0.80	0.64	1.27	1.97	1.86	2.19
	6	0.49	0.49	0.94	1.76	0.50	0.65	0.80	0.86	0.68	1.02	0.87	0.95	0.92
	7	0.50	0.50	0.94	1.53	0.48	0.77	0.95	1.07	0.82	0.94	1.00	1.03	1.00
	8	0.48	0.49	0.92	1.63	0.50	0.61	0.74	0.76	0.62	1.09	0.75	0.75	0.73
	9	0.50	0.50	0.96	1.85	0.52	0.63	0.76	0.79	0.64	0.87	0.71	0.78	0.84
	10	0.45	0.46	0.85	1.35	0.45	0.59	0.71	0.72	0.59	0.72	0.74	0.76	2.20
Average		0.49	0.49	0.93	1.66	0.49	0.65	0.79	0.83	0.66	0.98	1.16	1.01	1.28
Std. Dev. Of Max	1	0.57	0.15	0.65	2.27	0.15	0.26	0.51	0.65	0.29	0.65	0.91	1.70	0.71
	2	0.57	0.15	0.65	2.08	0.15	0.26	0.52	0.66	0.29	0.42	1.12	0.60	8.01
	3	0.55	0.15	0.64	1.98	0.14	0.27	0.53	0.66	0.30	0.32	3.36	1.84	0.98
	4	0.51	0.14	0.59	1.40	0.11	0.25	0.50	0.60	0.27	0.28	0.53	0.59	0.74
	5	0.60	0.16	0.67	2.42	0.17	0.26	0.51	0.62	0.28	0.25	0.54	2.64	1.67
	6	0.59	0.16	0.66	2.23	0.16	0.27	0.53	0.71	0.31	0.38	0.47	0.71	0.60
	7	0.59	0.16	0.65	1.77	0.14	0.33	0.67	1.02	0.43	0.35	0.54	0.76	0.61
	8	0.55	0.15	0.63	1.87	0.14	0.23	0.46	0.53	0.24	0.32	0.39	0.47	0.37
	9	0.58	0.15	0.66	2.28	0.16	0.24	0.48	0.59	0.27	0.45	0.28	0.45	0.54
	10	0.49	0.13	0.57	1.43	0.11	0.22	0.44	0.51	0.24	0.29	0.37	0.48	0.35
Average		0.56	0.15	0.64	1.97	0.14	0.26	0.51	0.66	0.29	0.37	0.85	1.02	1.46

*N-normal distribution, G-Gumbel distribution, L-lognormal distribution and W-Weibull distribution.

Table A-4. Projection test results of FC11 database (Normalized)

FC11	No.	Practical Method [Equation 3-6]	Linear models				Tail-linear models				Polynomial models			
			N*	G	L	W	N	G	L	W	N	G	L	W
Mean Of Max	1	0.57	0.58	1.11	2.47	0.63	0.68	0.78	0.79	0.69	0.76	0.78	0.81	0.78
	2	0.57	0.58	1.11	2.38	0.63	0.65	0.74	0.73	0.65	0.77	0.79	0.77	0.78
	3	0.58	0.59	1.14	2.49	0.65	0.63	0.71	0.70	0.62	0.77	0.80	0.81	1.15
	4	0.59	0.60	1.15	2.59	0.65	0.62	0.70	0.69	0.62	0.78	0.68	0.59	0.77
	5	0.56	0.56	1.06	1.91	0.57	0.72	0.82	0.84	0.73	0.97	0.86	0.75	0.84
	6	0.55	0.56	1.04	1.72	0.54	0.75	0.86	0.88	0.76	0.91	2.05	0.92	1.18
	7	0.57	0.58	1.08	1.85	0.57	0.79	0.91	0.94	0.80	1.05	1.16	0.98	1.07
	8	0.59	0.60	1.14	2.20	0.61	0.82	0.95	1.00	0.85	1.00	1.21	1.00	1.08
	9	0.58	0.59	1.11	2.09	0.60	0.76	0.88	0.89	0.77	1.28	0.90	0.94	1.23
	10	0.56	0.57	1.08	1.89	0.57	0.74	0.85	0.86	0.75	0.92	0.93	1.15	0.90
Average		0.57	0.58	1.10	2.16	0.60	0.72	0.82	0.83	0.72	0.92	1.01	0.87	0.98
Std. Dev. Of Max	1	0.39	0.09	0.39	1.70	0.11	0.13	0.23	0.27	0.14	0.11	0.17	0.21	0.18
	2	0.39	0.09	0.39	1.61	0.11	0.12	0.21	0.22	0.12	0.22	0.37	0.21	0.24
	3	0.40	0.10	0.40	1.71	0.11	0.11	0.19	0.19	0.10	0.19	0.24	0.27	0.83
	4	0.42	0.10	0.41	1.85	0.12	0.11	0.19	0.18	0.10	0.20	0.12	0.35	0.31
	5	0.37	0.09	0.37	1.17	0.09	0.14	0.25	0.30	0.16	0.49	0.24	0.24	0.21
	6	0.36	0.09	0.36	0.98	0.08	0.15	0.27	0.33	0.17	0.15	0.19	0.29	0.65
	7	0.37	0.09	0.37	1.10	0.08	0.17	0.30	0.37	0.19	0.25	0.24	0.29	0.49
	8	0.40	0.10	0.40	1.42	0.10	0.18	0.32	0.41	0.21	0.17	0.20	0.29	0.38
	9	0.39	0.09	0.39	1.32	0.09	0.16	0.28	0.33	0.17	0.22	0.22	0.32	1.18
	10	0.37	0.09	0.37	1.13	0.08	0.15	0.26	0.31	0.16	0.22	0.23	1.63	0.22
Average		0.39	0.09	0.38	1.40	0.10	0.14	0.25	0.29	0.15	0.22	0.22	0.41	0.47

*N-normal distribution, G-Gumbel distribution, L-lognormal distribution and W-Weibull distribution.

Table A-5 Projection test results of FC12 database (Normalized)

FC12	No.	Practical Method [Equation 3-6]	Linear models				Tail-linear models				Polynomial models			
			N*	G	L	W	N	G	L	W	N	G	L	W
Mean Of Max	1	0.56	0.57	1.06	1.99	0.57	0.81	0.93	0.98	0.83	0.96	1.01	0.98	1.07
	2	0.56	0.57	1.07	2.06	0.58	0.71	0.81	0.84	0.73	0.82	0.84	0.75	0.76
	3	0.56	0.57	1.06	2.04	0.58	0.65	0.73	0.74	0.65	1.76	0.88	0.78	0.85
	4	0.56	0.57	1.06	2.02	0.58	0.66	0.74	0.75	0.66	0.97	0.81	0.81	0.86
	5	0.56	0.57	1.06	1.97	0.57	0.63	0.71	0.71	0.63	0.93	1.52	0.66	1.32
	6	0.58	0.59	1.09	1.87	0.58	0.8	0.92	0.96	0.83	0.94	0.92	0.96	0.92
	7	0.59	0.6	1.12	2.04	0.61	0.8	0.92	0.97	0.83	0.95	1.01	0.89	1.23
	8	0.59	0.6	1.14	2.44	0.65	0.75	0.86	0.88	0.77	0.87	1.3	0.92	0.96
	9	0.6	0.61	1.13	2.23	0.63	0.78	0.9	0.94	0.81	0.82	0.94	0.85	0.88
	10	0.57	0.58	1.08	2.08	0.61	0.73	0.83	0.86	0.75	1.87	0.95	0.79	0.95
Average		0.57	0.58	1.09	2.07	0.6	0.73	0.83	0.86	0.75	1.09	1.02	0.84	0.98
Std. Dev. Of Max	1	0.61	0.15	0.59	2.09	0.16	0.29	0.50	0.65	0.34	0.21	0.31	0.48	0.45
	2	0.62	0.15	0.60	2.22	0.17	0.22	0.39	0.50	0.26	0.22	0.26	0.27	0.29
	3	0.60	0.15	0.59	2.17	0.17	0.19	0.33	0.35	0.19	0.43	0.36	0.33	0.30
	4	0.59	0.15	0.58	2.10	0.16	0.19	0.34	0.37	0.20	0.21	0.28	0.41	0.37
	5	0.60	0.15	0.59	2.07	0.16	0.17	0.31	0.31	0.17	0.24	0.21	0.27	0.63
	6	0.57	0.14	0.58	1.72	0.14	0.26	0.46	0.58	0.31	0.24	0.31	0.46	0.33
	7	0.59	0.15	0.60	1.93	0.15	0.26	0.45	0.59	0.31	0.27	0.42	0.51	0.62
	8	0.61	0.15	0.62	2.57	0.18	0.24	0.41	0.50	0.27	0.26	0.27	0.44	0.46
	9	0.60	0.15	0.61	2.24	0.16	0.25	0.44	0.56	0.30	0.22	0.45	0.30	0.39
	10	0.57	0.15	0.59	2.11	0.16	0.24	0.41	0.50	0.27	0.23	0.54	0.35	0.43
Average		0.6	0.15	0.59	2.12	0.16	0.23	0.4	0.49	0.26	0.25	0.34	0.38	0.43

*N-normal distribution, G-Gumbel distribution, L-lognormal distribution and W-Weibull distribution.

Appendix B: Projected live load statistics for moment and shear – Entire State - Gumbel

Each moment or shear location is identified in the following manner: The bridge ID in the leftmost column; In the column labeled "Load Effect.", and "M" indicates a moment in K-ft and a "V" indicates a shear in K. The first number after the m or v indicates the span number, and the second number indicates how far from the leftmost support for that span in terms of percent of the span. For example, for bridge no. B01-11072, the M14 indicates the moment on the first span at a location 40% from the leftmost support. The v20 indicates the negative shear at the second support.

Bridge		Load Effect	FC01		FC02		FC11		FC12		FC14	
Type	I.D.		Mean	Std	Mean	Std	Mean	Std	Mean	Std	Mean	Std
SC	S18-41064	M15	5536.50	358.60	5818.50	399.71	5828.69	375.44	5427.77	361.07	5405.80	386.63
		V10	157.67	10.25	166.00	11.44	165.81	10.72	151.45	10.09	153.98	11.06
	S20-41064	M15	4822.14	312.39	5026.45	343.55	5167.93	332.56	4722.23	312.45	4682.21	333.30
		V10	153.21	9.92	160.56	11.02	164.07	10.60	150.22	9.98	149.37	10.68
	B01-11072	M14	1397.63	85.10	1475.96	95.96	1410.19	83.39	1313.64	84.22	1331.03	86.90
		M20	947.26	60.86	1007.52	68.99	986.33	62.22	894.11	60.88	921.52	64.24
		V10	108.11	6.62	111.45	7.20	108.95	6.49	100.20	6.43	102.75	6.75
		V20	134.31	8.48	136.32	9.04	140.28	8.72	126.05	8.41	130.93	8.97
	S19-63174	M14	4422.03	285.06	4641.80	317.31	4676.03	297.19	4196.21	287.18	4366.33	306.42
		M20	2942.39	194.34	3155.67	222.10	3152.11	205.83	2814.31	198.23	2937.87	212.09
		M26	4990.43	326.10	5186.39	355.87	5219.75	332.94	4680.09	321.48	4872.61	343.22
		V10	149.59	9.66	156.28	10.68	157.88	10.05	141.43	9.69	147.56	10.37
		V20l	167.74	10.98	177.92	12.38	178.71	11.56	159.67	11.13	166.69	11.91
		V20r	171.01	11.23	182.16	12.72	182.40	11.83	163.19	11.41	170.12	12.20
		V30	152.03	9.84	159.37	10.93	160.70	10.26	143.91	9.89	150.16	10.59
	S03-19042	M20	2914.18	199.08	3228.85	226.91	3113.68	210.86	2906.71	202.98	2971.33	217.23
		M25	2887.93	190.23	3110.35	209.71	3024.94	196.55	2846.42	190.75	2891.40	202.65
		M30	1856.00	126.13	2035.17	141.99	1982.35	133.55	1849.39	128.42	1890.69	137.48
		M40	2973.52	203.18	3296.20	231.72	3177.06	215.20	2966.02	207.18	3031.90	221.71
		V20l	164.55	11.18	181.19	12.64	175.05	11.78	163.50	11.34	167.13	12.14
		V20r	149.73	10.04	161.89	11.10	158.23	10.50	147.89	10.10	151.15	10.82
		V30l	153.33	10.31	166.26	11.44	162.37	10.80	151.67	10.39	155.04	11.13
		V30r	152.81	10.27	165.67	11.40	161.79	10.76	151.15	10.36	154.50	11.09
		V40l	149.98	10.05	162.17	11.12	158.51	10.51	148.13	10.12	151.41	10.83
		V40r	165.21	11.23	182.02	12.71	175.78	11.83	164.18	11.39	167.83	12.20
		V50	145.21	9.70	157.03	10.74	152.92	10.10	143.11	9.74	146.25	10.43

Appendix B continued: Projected live load statistics for moment and shear– Entire State												
Type	I.D.	Load Effect	Mean	Std	Mean	Std	Mean	Std	Mean	Std	Mean	Std
PI	S11-19033	M15	4574.02	305.11	4949.88	338.13	4831.60	318.66	4525.57	307.64	4612.26	328.15
		V10	148.33	9.94	160.77	11.03	156.50	10.37	146.37	9.99	149.63	10.70
	B02-11052	M15	2909.49	182.02	3626.64	248.77	3231.80	204.25	3259.14	218.86	3113.92	214.06
		V10	124.83	7.84	155.99	10.73	137.94	8.74	139.46	9.39	133.21	9.18
	B04-11057	M15	4300.26	286.26	4644.76	316.52	4538.17	298.62	4252.49	288.41	4332.31	307.51
		V10	146.65	9.81	158.61	10.85	154.58	10.22	144.61	9.85	147.81	10.55
	B02-11112	M15	4095.13	272.14	4416.58	300.38	4318.09	283.59	4047.92	274.02	4122.31	292.02
		M25	3992.66	265.08	4302.87	292.34	4208.03	276.07	3945.79	266.83	4017.24	284.27
		V10	144.57	9.65	156.06	10.66	152.23	10.05	142.44	9.68	145.57	10.37
		V20	144.19	9.62	155.52	10.61	151.79	10.01	142.03	9.65	145.16	10.33
	R01-19034	M15	791.46	47.46	923.03	59.14	748.81	42.37	779.89	47.53	741.20	45.96
		M25	550.36	32.47	662.13	42.37	510.91	28.13	543.74	32.68	513.52	31.26
		V10	87.16	5.28	97.34	6.17	83.62	4.83	83.91	5.11	81.84	5.14
		V20	74.34	4.38	87.30	5.52	68.97	3.81	72.26	4.30	69.14	4.20
PCA	S05-82022	M15	2051.22	127.29	2125.75	139.78	2102.37	128.46	1935.77	126.91	1909.61	132.69
		V10	124.62	7.81	127.08	8.38	128.03	7.93	116.42	7.69	116.33	8.19
	S06-82022	M15	2051.22	127.29	2125.75	139.78	2072.60	128.46	1935.77	126.91	2027.98	132.69
		V10	124.62	7.81	127.08	8.38	126.19	7.93	116.42	7.69	123.63	8.19
	S25-82022	M15	3155.43	200.37	3265.16	219.16	3313.53	207.06	2986.47	200.91	3093.74	213.27
		V10	140.18	8.96	144.67	9.75	147.08	9.26	131.99	8.93	137.55	9.56
	S01-11015	M15	673.99	38.80	777.37	49.74	629.63	33.92	641.41	38.98	617.28	37.37
		V10	82.17	4.75	91.74	5.81	77.28	4.22	76.64	4.63	75.16	4.57
		M25	2291.14	143.13	2367.74	156.49	2377.14	145.60	2163.14	142.85	2223.88	150.22
		V20	128.15	8.08	130.97	8.69	133.05	8.24	119.99	7.98	124.62	8.51
		M45	845.83	49.30	952.59	61.06	803.34	44.22	802.51	49.33	777.72	47.78
		V40	89.09	5.25	96.99	6.18	85.51	4.81	82.81	5.10	82.11	5.12
	B02-46082	M15	800.93	48.06	932.80	59.78	758.55	42.98	789.16	48.13	750.27	46.57
		V10	86.84	5.26	97.16	6.17	83.28	4.82	83.66	5.10	81.53	5.12

Appendix B continued: Projected live load statistics for moment and shear– Entire State												
Type	I.D.	Load Effect	Mean	Std	Mean	Std	Mean	Std	Mean	Std	Mean	Std
PCS	B04-03072	M15	1217.21	72.84	1312.50	84.71	1200.55	69.09	1151.38	72.67	1139.45	72.55
		V10	105.40	6.39	108.96	7.00	105.48	6.21	97.60	6.20	99.52	6.46
	R01-55011	M15	2039.75	131.01	2182.24	143.68	2102.45	132.50	2002.95	130.65	2012.60	136.82
		V10	121.02	7.85	127.64	8.43	124.93	7.97	117.74	7.74	119.72	8.24
	S06-63081	M15	459.90	26.33	539.27	34.58	425.87	22.90	436.94	26.42	408.17	25.39
		M25	2154.84	134.12	2229.83	146.95	2214.52	135.84	2033.92	133.78	2010.04	140.22
		M35	481.90	27.56	565.60	36.25	445.05	23.88	458.75	27.73	427.37	26.56
		V10	72.10	4.08	83.22	5.24	66.17	3.50	67.85	4.03	63.83	3.92
		V20	125.84	7.91	128.48	8.49	129.50	8.04	117.68	7.80	117.61	8.31
		V30	73.25	4.15	84.32	5.31	67.28	3.57	68.85	4.09	64.82	3.99
	S14-33084	M15	736.69	42.59	842.54	53.94	687.35	37.55	722.47	42.73	667.66	41.10
		M25	2006.46	124.35	2081.03	136.71	2051.23	125.27	1957.48	123.96	1911.65	129.44
		M35	631.30	36.24	732.09	46.84	584.09	31.54	620.01	36.45	571.49	34.90
		V10	84.99	4.95	93.87	5.95	80.02	4.44	81.59	4.81	77.01	4.78
		V20	123.77	7.75	126.19	8.31	126.87	7.85	119.52	7.63	118.29	8.12
		V30	79.15	4.57	89.43	5.67	73.46	4.01	76.38	4.47	71.50	4.39
	B01-79031	M15	976.47	59.43	1110.57	71.38	942.67	54.74	960.29	59.35	921.99	58.28
		V10	93.64	5.77	102.36	6.54	91.62	5.44	90.10	5.59	88.89	5.71

Appendix C: Projected live load statistics for moment and shear – Entire State – Phase I Method

Each moment or shear location is identified in the following manner: The bridge ID in the leftmost column; In the column labeled "Load Effect.", and "M" indicates a moment in K-ft and a "V" indicates a shear in K. The first number after the m or v indicates the span number, and the second number indicates how far from the leftmost support for that span in terms of percent of the span. For example, for bridge no. B01-11072, the M14 indicates the moment on the first span at a location 40% from the leftmost support. The v20 indicates the negative shear at the second support.

Bridge		Load Effect	FC01		FC02		FC11		FC12		FC14	
Type	I.D.		Mean	Std	Mean	Std	Mean	Std	Mean	Std	Mean	Std
SC	S18-41064	M15	1620.42	326.54	1871.12	328.62	1645.00	299.84	1657.84	281.24	1693.66	296.18
		V10	45.77	9.44	52.98	9.40	46.38	8.70	46.78	8.07	47.86	8.63
	S20-41064	M15	1421.38	285.06	1455.64	272.36	1476.10	280.94	1451.00	241.38	1300.04	293.88
		V10	44.85	9.09	45.97	8.85	46.40	9.14	45.80	7.76	40.99	9.50
	B01-11072	M14	467.48	75.89	530.64	87.53	469.56	64.65	476.41	70.10	480.03	67.71
		M20	282.23	55.70	326.73	57.99	284.64	49.24	288.31	48.27	292.51	50.55
		V10	35.79	5.88	40.47	6.50	35.76	5.01	36.25	5.21	36.65	5.25
		V20	41.62	7.41	47.06	7.65	41.93	6.59	42.26	6.36	43.00	6.60
	S19-63174	M14	1308.78	258.42	1508.54	261.94	1327.40	235.80	1338.12	222.64	1366.06	233.56
		M20	820.89	182.46	961.70	182.24	835.29	171.01	842.99	157.99	864.06	168.42
		M26	1474.77	323.10	1672.12	293.22	1468.94	265.80	1480.96	250.08	1512.62	263.06
		V10	44.12	8.81	50.80	8.79	44.64	8.06	45.02	7.51	46.01	8.02
		V20l	47.82	10.20	55.63	10.15	48.54	9.48	48.97	8.76	50.15	9.37
		V20r	50.41	11.73	49.48	10.07	47.77	8.82	47.27	8.65	43.49	10.60
		V30	44.54	9.02	51.41	8.99	45.09	8.27	45.48	7.70	46.50	8.22
	S03-19042	M20	877.65	207.34	860.84	177.48	834.26	158.21	824.27	154.37	751.78	186.02
		M25	943.34	188.31	936.02	168.56	898.52	139.52	889.21	140.88	844.62	183.90
		M30	565.41	128.89	555.15	110.95	538.55	98.79	531.74	96.30	487.17	117.85
		M40	895.06	211.81	877.85	181.26	850.70	161.57	840.56	157.68	766.48	189.86
		V20l	50.28	11.65	49.36	10.00	47.66	8.76	47.16	8.59	43.41	10.55
		V20r	47.18	10.24	46.42	8.90	44.69	7.61	44.26	7.52	41.37	9.59
		V30l	48.00	10.54	47.21	9.13	45.50	7.87	45.04	7.74	41.95	9.82
		V30r	47.86	10.50	47.07	9.10	45.36	7.83	44.90	7.72	41.83	9.78
		V40l	47.25	10.26	46.50	8.91	44.76	7.62	44.33	7.53	41.43	9.60
		V40r	50.43	11.71	49.50	10.05	47.80	8.81	47.30	8.64	43.52	10.60
		V50	46.10	9.95	45.40	8.66	43.60	7.32	43.21	7.27	40.59	9.32

Appendix C continued: Projected live load statistics for moment and shear– Entire State												
Type	I.D.	Load Effect	Mean	Std	Mean	Std	Mean	Std	Mean	Std	Mean	Std
PI	S11-19033	M15	1399.72	218.88	1610.96	278.72	45.53	8.35	1430.96	237.56	1460.74	249.04
		V10	44.96	9.10	51.87	9.06	1023.60	157.76	45.91	7.76	46.95	8.29
	B02-11052	M15	998.55	184.61	1139.98	191.00	46.97	6.35	1019.02	160.21	1037.57	164.96
		V10	42.79	8.20	48.95	8.22	1341.04	235.12	43.57	6.97	44.49	7.40
	B04-11057	M15	1321.92	257.88	1519.34	261.36	45.17	8.20	1351.00	222.30	1378.64	232.52
		V10	44.62	8.96	51.41	8.92	1281.64	222.54	45.55	7.63	46.56	8.15
	B02-11112	M15	1263.56	244.56	1450.74	248.40	1252.00	216.28	1291.10	210.94	1317.08	167.47
		M25	1234.48	237.90	3657.00	242.00	44.66	8.04	1261.18	205.26	1286.38	214.04
		V10	44.14	8.80	50.79	8.76	44.62	8.00	45.03	7.49	46.03	6.29
		V20	44.09	8.76	50.72	8.73	295.25	38.67	44.98	7.46	45.97	7.95
	R01-19034	M15	296.80	45.58	340.96	57.88	209.66	27.19	303.43	45.74	300.98	43.43
		M25	211.22	31.76	245.32	42.64	31.86	4.11	215.92	33.01	213.87	31.44
		V10	32.20	4.94	36.59	5.98	28.21	3.62	32.65	4.70	32.59	4.58
		V20	28.65	4.35	33.04	5.54	45.53	8.35	29.14	4.32	28.88	4.18
PCA	S05-82022	M15	660.00	111.61	747.82	122.97	666.01	97.19	672.72	100.21	680.828	99.025
		V10	39.23	6.89	44.42	7.18	39.44	6.07	39.80	5.92	40.4702	6.1418
	S06-82022	M15	666.77	113.18	747.82	122.97	666.01	97.19	672.72	100.21	680.828	99.025
		V10	39.23	6.89	44.42	7.18	39.44	6.07	39.80	5.92	40.4702	6.1418
	S25-82022	M15	966.33	177.43	1102.32	184.25	978.74	159.22	985.98	154.24	1003.57	158.43
		V10	42.30	8.05	48.34	8.09	42.71	7.28	43.06	6.85	43.9452	7.2585
	S01-11015	M15	249.10	37.89	287.93	49.48	247.39	32.34	254.74	38.77	252.212	36.907
		V10	30.20	4.61	34.61	5.74	29.77	3.84	30.67	4.49	30.4786	4.3559
		M25	727.00	125.48	824.65	135.84	734.49	110.21	741.07	111.44	751.353	111.33
		V20	39.87	7.15	45.24	7.37	40.13	6.34	40.48	6.12	41.2033	6.3871
		M45	306.50	47.12	351.67	59.56	305.06	39.90	313.28	47.11	310.999	44.662
		V40	31.69	4.93	36.16	5.96	31.33	4.08	32.17	4.69	32.0989	4.53
	B02-46082	M15	300.01	46.10	344.50	58.43	298.49	39.08	306.69	46.20	304.283	43.84
		V10	32.02	4.93	36.49	5.97	31.67	4.10	32.47	4.69	32.4136	4.559

Appendix C continued: Projected live load statistics for moment and shear– Entire State												
Type	I.D.	Load Effect	Mean	Std	Mean	Std	Mean	Std	Mean	Std	Mean	Std
PCS	B04-03072	M15	421.07	66.24	478.44	79.54	421.55	55.89	429.68	63.41	429.93	60.27
		V10	35.51	5.68	40.05	6.43	38.60	4.85	35.95	5.13	36.25	5.09
	R01-55011	M15	675.75	114.83	765.84	125.98	682.11	100.22	688.78	102.82	697.40	101.87
		V10	39.27	6.93	44.49	7.21	39.48	6.11	39.85	5.95	40.52	6.18
	S06-63081	M15	170.97	25.17	199.16	35.04	170.03	21.54	174.41	26.54	173.67	25.19
		M25	689.02	117.56	781.05	128.51	695.68	102.76	702.31	105.04	711.38	104.27
		M35	179.49	26.57	209.08	36.72	178.25	22.76	183.26	27.96	181.99	26.60
		V10	27.43	4.07	31.70	5.35	27.03	3.39	27.87	4.10	27.64	4.00
		V20	39.41	6.99	44.67	7.25	39.63	6.17	40.00	5.99	40.68	6.23
		V30	27.81	4.14	32.11	5.40	27.40	3.45	28.26	4.16	28.02	4.06
	S14-33084	M15	270.47	41.34	311.75	53.26	268.79	35.19	276.58	41.92	274.00	39.87
		M25	647.42	109.05	733.45	120.60	653.15	94.80	659.90	98.15	667.59	96.78
		M35	234.20	35.50	271.26	46.81	232.49	30.36	239.50	36.54	237.05	34.82
		V10	30.86	4.74	35.29	5.83	30.46	3.94	31.34	4.57	31.19	4.43
		V20	39.06	6.83	44.22	7.14	39.26	6.01	39.63	5.88	40.28	6.09
		V30	29.20	4.49	33.64	5.63	28.76	3.72	29.71	4.41	29.47	4.25
	B01-79031	M15	357.44	55.47	407.96	68.44	356.65	46.79	365.09	54.35	363.63	51.51
		V10	33.51	5.25	37.98	6.17	33.27	4.38	33.97	4.87	34.06	4.76

Appendix D: Calculated dead load moment and shear effect for the bridges in this study

	Bridge #	Load Effect	Dead Load Effect (m: k-ft; v: k)
SC	S18-41064	m15	6171
		v10	122.1
	S20-41064	m15	2831.95
		v10	74.8
	B01-11072	m14	376.5
		m20	669.33
		v10	25.6
		v20	47
	S19-63174	m14	2258.5
		m20	4960.8
		m26	3246.4
		v10	60.5
		v20l	112.4
		v20r	120.3
		v30	70.6
	S03-19042	m20	3841.5
		m25	754.9
		m30	1471.5
		m40	3918.5
		v20l	94.5
		v20r	85.3
		v30l	67.1
		v30r	67.1
		v40l	85.3
		v40r	94.5
		v50	69.3

	Bridge #	Load Effect	Dead Load Effect (m: k-ft; v: k)
PI	S11-19033	m15	3653
		v10	158.4
	B01-11052	m15	2204
		m25	2220
		m35	2220
		m45	2220
		v10	94
		v20	94.4
		v30	94.4
		v40	94.4
	B04-11057	m15	3731.7
		m25	3731.7
		v10	161.1
		v20	160.1
	B02-11112	m15	3145
		m25	3145
		m45	3145
		v10	154.2
		v20	151.3
		v40	152
	R01-19034	m15	328.25
		m25	210
		v10	34.7
		v20	27.5

	Bridge #	Load Effect	Dead Load Effect (m: k-ft; v: k)
PCS	B04-03072	m15	439.4
		v10	42.3
	R01-55011	m15	1093.7
		v10	60.1
	S06-63081	m15	156.3
		m25	1054.5
		m35	167.4
		v10	22
		v20	57.1
		v30	22.8
	S14-33084	m15	277.7
		m25	937.2
		m35	229.4
		v10	28.9
		v20	53.1
		v30	26.3
	B01-79031	m15	466.8
		v10	40.1

	Bridge #	Load Effect	Dead Load Effect (m: k-ft; v: k)
PCA	S05-82022	m15	601.1
		v10	33.6
	S06-82022	m15	601.1
		v10	33.6
	S25-82022	m15	1208.7
		v10	50.6
	S01-11015	m15	154.6
		v10	17
		m25	688.2
		v20	35.8
		m45	204.8
		v40	19.6
	B02-46082	m15	176.4
		v10	17.1

Appendix E: Moment and shear capacities (m in ft-kips, v in kips)

	Bridge I.D.	Load effect	Capacity	Governing load
SC	S18-41064	m15	14651.4	Truck + Lane
		v10	364.9	Truck + Lane
	S20-41064	m15	8149.9	Truck + Lane
		v10	248.1	Truck + Lane
	B01-11072	m14	1759.9	Truck + Lane
		m20	2153.8	Truck + Lane
		v10	165.2	Truck + Lane
		v20	258.3	Truck + Lane
	S19-63174	m14	6613.2	Truck + Lane
		m20	10299.5	Truck + Lane
		m26	8426.4	Truck + Lane
		v10	234.8	Truck + Lane
		v20l	411.8	Truck + Lane
		v20r	422.3	Truck + Lane
		v30	245.3	Truck + Lane
	S03-19042	m20	8302.8	Truck + Lane
		m25	3141.2	Truck + Lane
		m30	4036.3	Truck + Lane
		m40	8446.4	Truck + Lane
		v20l	493.5	Truck + Lane
		v20r	478.9	Truck + Lane
		v30l	412.2	Truck + Lane
		v30r	412.2	Truck + Lane
		v40l	474.1	Truck + Lane
		v40r	488.3	Truck + Lane
		v50	339.9	Truck + Lane

	Bridge #	Load effect	Capacity	Governing load
PI	S11-19033	m15	10114.026	Truck + Lane
		v10	376.069	Truck + Lane
	B01-11052	m15	6501.826	Truck + Lane
		v10	281.548	Truck + Lane
	B04-11057	m15	10417.177	Truck + Lane
		v10	392.027	Truck + Lane
	B02-11112	m15	9405.493	Truck + Lane
		m25	9285.804	Truck + Lane
		v10	386.636	Truck + Lane
		v20	381.564	Truck + Lane
	R01-19034	m15	1717.060	Truck + Lane
		m25	922.604	Truck + Lane
		v10	179.229	Truck + Lane
		v20	157.448	Truck + Lane

	Bridge I.D.	Load effect	Capacity	Governing load
PCS	B04-03072	m15	1552.195	Truck + Lane
		v10	167.778	Truck + Lane
	R01-55011	m15	3018.294	Truck + Lane
		v10	217.130	Truck + Lane
	S06-63081	m15	692.171	Tandem + Lane
		m25	2860.752	Truck + Lane
		m35	724.260	Tandem + Lane
		v10	120.190	Truck + Lane
		v20	206.907	Truck + Lane
		v30	122.978	Truck + Lane
	S14-33084	m15	1000.249	Tandem + Lane
		m25	2579.767	Truck + Lane
		m35	878.866	Tandem + Lane
		v10	138.582	Truck + Lane
		v20	193.130	Truck + Lane
		v30	131.174	Truck + Lane
	B01-79031	m15	1607.191	Truck + Lane
		v10	180.070	Truck + Lane

	Bridge I.D.	Load eff.	Capacity	Governing load
PCA	S05-82022	m15	1441.142	Truck + Lane
		v10	134.413	Truck + Lane
	S06-82022	m15	1441.142	Truck + Lane
		v10	134.413	Truck + Lane
	S25-82022	m15	2539.628	Truck + Lane
		v10	155.560	Truck + Lane
	S01-11015	m15	487.017	Tandem + Lane
		v10	95.632	Truck + Lane
		m25	1562.433	Truck + Lane
		v20	142.353	Truck + Lane
		m45	589.836	Truck + Lane
		v40	103.125	Truck + Lane
	B02-46082	m15	557.144	Truck + Lane
		v10	94.871	Truck + Lane

Appendix F: Projected live load statistics for moment and shear – Metro Region – Phase I Method

Each moment or shear location is identified in the following manner: The bridge ID in the leftmost column; In the column labeled "Load Effect.", and "M" indicates a moment in K-ft and a "V" indicates a shear in K. The first number after the m or v indicates the span number, and the second number indicates how far from the leftmost support for that span in terms of percent of the span. For example, for bridge no. B01-11072, the M14 indicates the moment on the first span at a location 40% from the leftmost support. The v20 indicates the negative shear at the second support.

Bridge		Load Effect	FC01		FC02		FC11		FC12		FC14	
Type	I.D.		Mean	Std	Mean	Std	Mean	Std	Mean	Std	Mean	Std
SC	S18-41064	M15	5054	14.4	5402.8	302	7544.6	16.4	7712.6	76.5	4610.8	45.1
		V10	140.28	0.12	177.68	5.62	212.6	2	220.9	1.91	130.8	1.26
	S20-41064	M15	4394.1	11.5	5499	221.9	6551.6	9.08	6692	68.9	4030.2	37.7
		V10	136.72	0.02	173	8.34	208.2	1.4	215.3	1.98	128.6	1.18
	B01-11072	M14	1273	2.94	1518	54.5	2001.4	5.3	1955.6	18.5	1222	3.42
		M20	1022.1	0.11	1313	58.1	1522	1.89	1588.1	33.2	975.3	4.04
		V10	96.8	0.24	124.8	4.38	158.7	0.23	158.4	1.86	97.6	0.24
		V20	159.8	0.49	211.2	13.4	240.6	0.91	244.5	1.57	143.3	1.62
	S19-63174	M14	4035.3	10.4	5061.3	188	6055.1	16.8	6169.2	28.4	3720	33
		M20	2703.8	6.14	3508.7	184.1	4015.8	20.4	4063.7	26	2388	26.6
		M26	4506.6	12.15	5668	198.8	6756.6	22.3	6862.7	32.4	4132.5	38.3
		V10	133.4	0.014	169.7	7.38	205.1	1.16	210.1	0.74	126.6	1.09
		V20l	149.9	0.23	194.4	9.55	227.5	1.79	230	0.95	137.6	1.42
		V20r	153	0.29	200.8	11.1	231.6	1.75	233.8	1.02	139.4	1.48
		V30	136.4	0.06	173.4	7.32	208.9	1.47	214.2	0.84	128.5	1.17
	S03-19042	M20	2751.7	7.12	3561.4	200	3995.4	56.1	4170.3	36	2443.4	27.4
		M25	2740	6.15	3340.3	87.4	4026.8	22.7	4131.5	47.3	2557.6	20.2
		M30	1727	5.12	2236.9	137.6	2535.3	35.9	2646.6	24.9	1560.7	17.04
		M40	2810.2	7.17	3632.9	200.2	4077.6	57.3	4254.8	36.6	2493.5	27.9
		V20l	152.06	0.29	197.5	10.6	225.8	2.61	234.8	1.97	139	1.48
		V20r	137.48	0.008	173.3	7.33	206.5	2.05	215	2.06	129.8	1.16
		V30l	140.49	0.044	177.2	8.13	209.9	2.05	219.6	2.07	131.9	1.23
		V30r	139.9	0.065	176.1	7.66	209.4	2.1	218.7	2.05	131.5	1.2
		V40l	137.76	0.03	173.9	7.34	207	2.03	216.4	2.08	130.1	1.17
		V40r	152.2	0.29	197.6	10.8	225.9	2.58	234.8	1.97	139.1	1.49
		V50	133.86	0.005	168.8	7.04	201.6	1.9	210.5	1.95	126.7	1.12

Appendix F continued: Projected live load statistics for moment and shear– Metro Region												
Type	I.D.	Load Effect	Mean	Std	Mean	Std	Mean	Std	Mean	Std	Mean	Std
PI	S11-19033	M15	4324.5	11.5	5392.3	216.6	6329.3	57.6	6545.7	69.1	3975.5	36.7
		V10	136.8	0	172.3	7.63	204.5	2.13	213.6	2.01	128.4	1.21
	B02-11052	M15	3019.1	5.78	3640.4	27.6	4442.2	22.3	4562.1	54.6	2824.2	22.2
		V10	125.8	0.029	160.4	7.69	192	1.62	199.5	1.91	121.8	0.95
	B04-11057	M15	4099.9	10.51	5085.4	190	6002.7	50.8	6201	66.4	3777.6	34.2
		V10	134.77	0.016	170.6	7.93	202.8	2.08	211.8	1.95	127.4	1.13
	B02-11112	M15	3876.3	7.53	4780.4	166.3	5679.9	44.1	5860.8	63.9	3580.3	31.7
		M25	3789.9	9.15	4653.5	137.2	5555.3	41.5	5729.9	63	3504.1	30.8
		V10	132.58	0.051	168.3	7.75	201	1.87	208.7	2.02	126.4	1.1
		V20	131.98	0.05	167.3	7.24	200.2	1.85	207.8	2.03	126	1.09
	R01-19034	M15	742.2	0.2	939.9	58.5	1338.5	2.87	1210.8	18.9	754.3	1.57
		M25	501.4	0.63	631.3	35.5	928	6.16	814.4	14.1	508	1.6
		V10	81.4	0.35	109.3	5.64	144.2	0.6	135.9	1.23	81.4	0.15
		V20	70.96	0.12	91.8	4.09	131.5	0.36	116.4	0.4	68.5	0.21
PCA	S05-82022	M15	1941.8	0.11	2401.1	97.7	2985.7	2.28	2900.9	19.6	1862.2	10.1
		V10	112.2	0.145	143.7	4.6	176.2	0.91	169	1.45	110.9	0.67
	S06-82022	M15	1930.6	0.18	2390.1	99.9	2950.7	16.85	2887.8	19.4	1856.3	9.72
		V10	112.3	0.15	143.6	4.7	174.7	1.08	169.1	1.45	111	0.58
	S25-82022	M15	2899.2	4.95	3608.7	134.6	4302	7.36	4260.8	30.8	2714.9	20.9
		V10	124.4	0.002	159.8	7	193.2	0.07	188.3	1.13	120.5	0.91
	S01-11015	M15	618.9	0.004	767.7	37.2	1139	2.27	979.2	9.87	622	2.54
		V10	76.4	0.28	101.4	6	140.5	0.19	125.2	0.35	76	0.04
		M25	2131.6	1.15	2626.9	101.4	3239	2.12	3144	24	2032.7	12.3
		V20	114.9	0.085	147.1	4.9	180.9	1.06	173.2	1.33	113.4	0.68
		M45	775.6	0.24	968.8	50.5	1109.3	2.67	950.7	9.61	601.7	2.72
		V40	84.5	0.23	113.3	8.7	138.7	0.28	123.3	0.33	74.7	0.15
	B02-46082	M15	751.68	0.21	930	45.6	1354.2	2.94	1285.2	4.05	764.4	1.44
		V10	82.9	0.24	110.7	8.78	144.8	0.65	136.7	0.29	81.4	0.14

Appendix F continued: Projected live load statistics for moment and shear– Metro Region												
Type	I.D.	Load Effect	Mean	Std	Mean	Std	Mean	Std	Mean	Std	Mean	Std
PCS	B04-03072	M15	1092	0.55	1393.1	75.5	1873	0.8	1815.4	5.27	1114	0.038
		V10	94.6	0.37	124.6	6.4	156.5	0.16	154.5	1.3	95.7	0.12
	R01-55011	M15	1932.3	0.18	2420.2	126.1	2944.3	17	2976	34.2	1853.3	10.1
		V10	112.7	0.15	142	4.7	174.4	1.09	171.7	2.22	110.7	0.6
	S06-63081	M15	399.2	0.55	484.6	25.1	765.2	3.96	621	11.6	422.1	0.47
		M25	1979.4	0.13	2436.6	108.9	3030.4	17.1	2988.2	36.7	1895.4	10.5
		M35	418.9	0.78	517.5	28.2	806	4.63	664.9	12.3	447.7	0.04
		V10	65.8	0.11	87.5	6.5	125.9	0.37	105.6	0.31	64.1	0.14
		V20	112.9	0.13	143.8	4.5	177	0.93	171.4	2.27	111.5	0.69
		V30	67.2	0.1	89.5	6.9	127.4	0.43	108.3	0.28	64.7	0.2
	S14-33084	M15	668.69	0.07	830.8	49.5	1219.1	2.1	1113.9	18.4	675.2	2.14
		M25	1835.1	0.78	2275.6	105.8	2857.7	2.32	2895.9	30.1	1770.7	9.1
		M35	569.47	0.18	725.2	47	1021.1	3.9	914.6	15.4	547.8	2.66
		V10	78.8	0.2	103.9	6.7	142.3	0.51	132.05	0.02	77.9	0.11
		V20	110.36	0.163	141	4.6	174.5	1.19	181.4	0.32	109.6	0.57
		V30	73.6	0.264	96.7	4.9	135.4	0.24	121.69	0.16	71.8	0.17
	B01-79031	M15	911.3	0.58	1151.6	55.3	1607.7	1.68	1530.6	4.7	925.6	0.73
		V10	89.1	0.288	117.8	8.3	149.9	0.75	145.4	0.71	88.7	0.003

Appendix G: Reliability indices without additional live load factor for Metro Region

Bridge		Load Effect	FC01	FC02	FC11	FC12	FC14
Type	I.D.		Design Min	Design Min	Design Min	Design Min	Design Min
SC	S18-41064	M15	3.63		2.75	3.78	3.78
		V10	3.56		2.11	2.84	3.75
	S20-41064	M15	3.84		2.72	3.79	4.03
		V10	3.14		1.44	1.92	3.35
	B01-11072	M14	3.74		1.80	2.93	3.89
		M20	4.08		2.89	3.98	4.19
		V10	3.47		1.07	1.75	3.42
		V20	3.12		1.17	1.73	3.57
	S19-63174	M14	3.70		2.46	3.43	3.89
		M20	3.86		3.38	4.79	3.98
		M26	3.70		2.66	3.70	3.87
		V10	3.24		1.40	1.96	3.43
		V20l	4.57		3.26	4.80	4.78
		V20r	4.48		3.19	4.68	4.70
		V30	3.09		1.32	1.82	3.31
	S03-19042	M20	4.11		3.43	4.78	4.28
		M25	3.69		1.97	2.95	3.95
		M30	4.74		3.80	5.45	4.93
		M40	4.11		3.44	4.80	4.28
		V20l	4.93		3.53	5.29	5.19
		V20r	5.26		3.89	5.94	5.42
		V30l	4.85		3.29	4.95	5.05
		V30r	4.86		3.30	4.98	5.06
		V40l	5.25		3.88	5.90	5.41
		V40r	4.92		3.52	5.28	5.18
		V50	4.00		2.29	3.31	4.20

Appendix G continued: Reliability indices without additional live load factor for Metro Region							
Type	I.D.	Load Effect	FC01	FC02	FC11	FC12	FC14
PI	S11-19033	M15	4.23		2.87	4.07	4.47
		V10	3.07		2.28	2.86	3.17
	B02-11052	M15	4.15		2.60	3.73	4.37
		V10	3.13		2.06	2.58	3.20
	B04-11057	M15	4.25		2.88	4.09	4.49
		V10	3.13		2.32	2.94	3.22
	B02-11112	M15	4.34		2.85	4.06	4.59
		M25	4.29		2.82	4.02	4.54
		V10	3.12		2.26	2.86	3.20
		V20	3.12		2.25	2.84	3.20
	R01-19034	M15	4.93		1.53	3.53	4.85
		M25	5.38		1.72	4.27	5.31
		V10	3.76		2.03	3.12	3.76
		V20	3.88		1.99	3.37	3.96
PCA	S05-82022	M15	3.81		2.11	3.31	3.95
		V10	2.81		1.25	1.83	2.85
	S06-82022	M15	3.83		2.17	3.34	3.95
		V10	2.81		1.29	1.83	2.84
	S25-82022	M15	3.71		2.49	3.70	3.87
		V10	2.93		1.68	2.28	3.00
	S01-11015	M15	4.24		1.08	2.97	4.22
		V10	3.15		0.84	1.77	3.16
		M25	3.83		2.34	3.62	3.96
		V20	2.76		1.17	1.73	2.79
		M45	4.03		2.38	4.71	4.97
		V40	3.03		1.20	2.25	3.38
	B02-46082	M15	5.88		3.02	5.43	5.82
		V10	4.01		2.31	3.61	4.05

Appendix G continued: Reliability indices without additional live load factor for Metro Region							
	I.D.	Load Effect	FC01	FC02	FC11	FC12	FC14
PCS	B04-03072	M15	4.61		1.80	3.07	4.52
		V10	3.43		1.88	2.56	3.39
	R01-55011	M15	4.63		2.95	4.40	4.77
		V10	3.20		1.93	2.63	3.23
	S06-63081	M15	5.14		1.37	4.25	4.86
		M25	4.59		2.89	4.41	4.73
		M35	5.15		1.39	4.10	4.82
		V10	3.50		1.25	2.65	3.57
		V20	3.10		1.75	2.44	3.14
		V30	3.50		1.29	2.63	3.60
	S14-33084	M15	4.79		1.58	3.30	4.74
		M25	4.65		2.87	4.19	4.77
		M35	4.92		1.74	3.75	5.09
		V10	3.44		1.48	2.36	3.46
		V20	3.13		1.75	2.08	3.14
		V30	3.50		1.48	2.54	3.56
	B01-79031	M15	5.11		2.34	3.99	5.05
		V10	3.63		2.12	2.95	3.63

Appendix H: Reliability indices without additional live load factor for Entire State

Bridge		Load Effect	FC01	FC02	FC11	FC12	FC14
Type	I.D.		Design Min	Design Min	Design Min	Design Min	Design Min
SC	S18-41064	M15	4.75	4.66	4.75	4.75	4.73
		V10	5.40	5.24	5.40	5.40	5.37
	S20-41064	M15	5.30	5.29	5.27	5.30	5.37
		V10	5.40	5.38	5.36	5.41	5.50
	B01-11072	M14	5.97	5.73	6.00	5.96	5.96
		M20	5.77	5.65	5.77	5.76	5.75
		V10	6.14	5.85	6.19	6.15	6.13
		V20	6.49	6.30	6.50	6.50	6.47
	S19-63174	M14	5.29	5.16	5.29	5.29	5.26
		M20	4.50	4.45	4.50	4.50	4.49
		M26	5.00	4.91	5.02	5.01	5.00
		V10	5.67	5.46	5.68	5.69	5.64
		V20l	6.17	6.03	6.17	6.17	6.14
		V20r	6.02	6.06	6.11	6.12	6.15
		V30	5.47	5.26	5.47	5.48	5.43
	S03-19042	M20	5.07	5.09	5.11	5.11	5.15
		M25	6.16	6.21	6.32	6.34	6.33
		M30	5.96	5.99	6.02	6.03	6.07
		M40	5.05	5.07	5.09	5.09	5.13
		V20l	6.72	6.77	6.83	6.84	6.88
		V20r	6.90	6.94	7.00	7.01	7.03
		V30l	6.80	6.86	6.94	6.95	6.97
		V30r	6.81	6.87	6.94	6.95	6.97
		V40l	6.89	6.93	6.99	7.00	7.02
		V40r	6.70	6.75	6.81	6.82	6.86
		V50	6.20	6.27	6.36	6.38	6.39

Appendix H continued: Reliability indices without additional live load factor for Entire State							
Type	I.D.	Load Effect	FC01	FC02	FC11	FC12	FC14
PI	S11-19033	M15	6.14	5.95	6.11	6.11	6.08
		V10	4.08	3.99	4.08	4.07	4.06
	B02-11052	M15	6.26	6.08	6.26	6.26	6.23
		V10	4.40	4.30	4.35	4.40	4.38
	B04-11057	M15	6.14	5.99	6.15	6.15	6.12
		V10	4.14	4.05	4.13	4.13	4.12
	B02-11112	M15	6.38	6.21	6.39	6.39	6.40
		M25	6.33	4.07	6.33	6.33	6.30
		V10	4.18	4.09	4.17	4.17	4.16
		V20	4.18	4.09	4.18	4.18	4.16
	R01-19034	M15	7.59	7.11	7.68	7.54	7.58
		M25	5.95	5.24	6.07	5.86	5.92
		V10	5.03	4.88	5.05	5.02	5.02
		V20	5.13	4.95	5.16	5.11	5.12
PCA	S05-82022	M15	5.83	5.65	5.84	5.83	5.81
		V10	4.55	4.40	4.56	4.55	4.53
	S06-82022	M15	5.82	5.65	5.84	5.83	5.81
		V10	4.55	4.40	4.56	4.55	4.53
	S25-82022	M15	5.29	5.16	5.29	5.29	5.27
		V10	4.36	4.24	4.36	4.36	4.33
	S01-11015	M15	6.57	6.15	6.63	6.52	6.55
		V10	4.79	4.57	4.84	4.78	4.79
		M25	5.63	5.47	5.63	5.62	5.61
		V20	4.53	4.37	4.54	4.53	4.50
		M45	6.27	5.92	6.33	6.23	6.26
		V40	4.77	4.57	4.81	4.76	4.77
	B02-46082	M15	7.92	7.58	7.97	7.88	7.91
		V10	5.33	5.17	5.35	5.32	5.32

Appendix H continued: Reliability indices without additional live load factor for Entire State							
Type	I.D.	Load Effect	FC01	FC02	FC11	FC12	FC14
PCS	B04-03072	M15	7.05	6.72	7.11	7.03	7.05
		V10	4.82	4.68	4.74	4.81	4.80
	R01-55011	M15	6.62	6.43	6.63	6.62	6.60
		V10	4.62	4.50	4.62	4.62	4.60
	S06-63081	M15	7.57	6.97	7.66	7.50	7.53
		M25	6.55	6.37	6.56	6.55	6.53
		M35	7.53	6.95	7.62	7.46	7.50
		V10	4.88	4.66	4.92	4.86	4.88
		V20	4.58	4.46	4.59	4.58	4.56
		V30	4.88	4.67	4.92	4.87	4.88
	S14-33084	M15	7.14	6.71	7.21	7.09	7.13
		M25	6.61	6.42	6.62	6.60	6.59
		M35	7.29	6.81	7.37	7.23	7.28
		V10	4.84	4.66	4.87	4.83	4.84
		V20	4.58	4.46	4.59	4.58	4.56
		V30	4.88	4.69	4.92	4.87	4.88
	B01-79031	M15	7.27	6.95	7.32	7.24	7.26
		V10	4.92	4.79	4.94	4.92	4.92

Appendix I: Reliability indices with additional live load factor of 1.2 for Metro Region

Bridge		Load Effect	FC01	FC02	FC11	FC12	FC14
Type	I.D.		Design Min	Design Min	Design Min	Design Min	Design Min
SC	S18-41064	M15	3.94		3.04	2.98	4.10
		V10	3.92		2.47	2.32	4.11
	S20-41064	M15	4.20		3.06	2.99	4.39
		V10	3.52		1.82	1.67	3.73
	B01-11072	M14	4.16		2.22	2.33	4.31
		M20	4.45		3.26	3.10	4.57
		V10	3.92		1.54	1.55	3.88
		V20	3.57		1.62	1.54	4.01
	S19-63174	M14	4.05		2.79	2.73	4.24
		M20	4.15		3.66	3.64	4.27
		M26	4.03		2.97	2.92	4.20
		V10	3.64		1.80	1.69	3.83
		V20l	4.94		3.65	3.61	5.15
		V20r	4.85		3.58	3.54	5.07
		V30	3.48		1.70	1.59	3.69
	S03-19042	M20	4.45		3.74	3.66	4.62
		M25	4.10		2.39	2.30	4.36
		M30	5.10		4.16	4.05	5.29
		M40	4.44		3.75	3.67	4.61
		V20l	5.31		3.96	3.83	5.56
		V20r	5.64		4.32	4.20	5.79
		V30l	5.24		3.74	3.58	5.44
		V30r	5.26		3.75	3.60	5.45
		V40l	5.62		4.31	4.18	5.77
		V40r	5.30		3.95	3.83	5.55
		V50	4.41		2.73	2.58	4.60

Appendix I continued: Reliability indices with additional live load factor of 1.2 for Metro Region							
Type	I.D.	Load Effect	FC01	FC02	FC11	FC12	FC14
PI	S11-19033	M15	4.72		3.33	3.20	4.97
		V10	3.29		2.49	2.41	3.39
	B02-11052	M15	4.65		3.06	2.97	4.88
		V10	3.38		2.33	2.25	3.45
	B04-11057	M15	4.74		3.34	3.22	4.99
		V10	3.35		2.55	2.47	3.44
	B02-11112	M15	4.84		3.33	3.20	5.10
		M25	4.80		3.29	3.17	5.05
		V10	3.35		2.49	2.42	3.43
		V20	3.35		2.48	2.41	3.43
	R01-19034	M15	5.53		2.11	2.80	5.45
		M25	4.96		1.20	2.13	4.88
		V10	4.04		2.39	2.63	4.03
		V20	4.16		2.35	2.79	4.23
PCA	S05-82022	M15	4.28		2.54	2.67	4.43
		V10	3.11		1.59	1.75	3.15
	S06-82022	M15	4.30		2.59	2.69	4.43
		V10	3.11		1.63	1.75	3.14
	S25-82022	M15	4.14		2.87	2.91	4.30
		V10	3.19		1.96	2.05	3.26
	S01-11015	M15	4.79		1.58	2.46	4.77
		V10	3.46		1.24	1.73	3.47
		M25	4.29		2.75	2.87	4.42
		V20	3.06		1.51	1.68	3.09
		M45	4.57		2.88	3.65	5.51
		V40	3.35		1.59	2.06	3.67
	B02-46082	M15	6.46		3.61	4.07	6.40
		V10	4.29		2.68	2.93	4.33

Appendix I continued: Reliability indices with additional live load factor of 1.2 for Metro Region							
Type	I.D.	Load Effect	FC01	FC02	FC11	FC12	FC14
PCS	B04-03072	M15	5.18		2.34	2.52	5.09
		V10	3.71		2.22	2.27	3.68
	R01-55011	M15	5.16		3.45	3.44	5.30
		V10	3.47		2.24	2.30	3.50
	S06-63081	M15	5.75		1.96	3.27	5.47
		M25	5.11		3.39	3.45	5.26
		M35	5.75		1.98	3.18	5.42
		V10	3.80		1.63	2.33	3.86
		V20	3.38		2.06	2.17	3.42
		V30	3.80		1.68	2.32	3.89
	S14-33084	M15	5.36		2.13	2.67	5.32
		M25	5.18		3.37	3.30	5.30
		M35	5.50		2.30	2.97	5.67
		V10	3.72		1.85	2.13	3.75
		V20	3.40		2.06	1.92	3.42
		V30	3.79		1.85	2.26	3.85
	B01-79031	M15	5.68		2.89	3.15	5.62
		V10	3.90		2.45	2.52	3.91